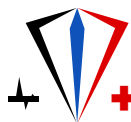




## Project Deliverable

<b>Project Number:</b> 325275	<b>Project Acronym:</b> SAPPHIRE	<b>Project Title:</b> System Automation of PEMFCs with Prognostics and Health management for Improved Reliability and Economy
<b>Instrument:</b> Collaborative Project (CP)		<b>Thematic Priority:</b> Fuel Cells and Hydrogen Joint Undertaking
<b>Title:</b>  <b>Tests and performance evaluation of prognostic approaches</b>		
<b>Contractual Delivery Date:</b> April 30, 2016		<b>Actual Delivery Date:</b> May 30, 2016
<b>Start Date of the Project:</b> May 1, 2013		<b>Duration:</b> 36 months
<b>Organisation name of lead contractor for this deliverable:</b> FCLAB		<b>Document Version:</b> 2.0
<b>Organisation notes:</b>		

Dissemination level (Project co-funded by the European Commission within the Seventh Framework Programme)		
<b>PU</b>	Public	<b>PU</b>  Public
<b>PP</b>	Restricted to other programme participants (including the Commission)	
<b>RE</b>	Restricted to a group defined by the consortium (including the Commission)	
<b>CO</b>	Confidential, only for members of the consortium (including the Commission)	

**Authors (organisations):**

Elodie Lechartier (FCLAB), Christoph Kaendler (EIFER)

**Abstract:**

This deliverable aims at validating the two prognostics approaches developed. The validation is realized thanks to data gathered during the lasting of the project.

**Keywords:**

prognostics, Hyrbid, SAPPHIRE

## Revision History

Rev.	Date	Description	Author (organisation)
1.0	2015/04/04	First version (FCLAB)	Elodie Lechartier (FCLAB)
1.1	2015/05/20	Corrections (FCLAB)	Elodie Lechartier (FCLAB)
1.2	2015/05/25	First version (EIFER)	Christoph Kaendler (EIFER)
1.2	2015/05/27	First revision (EIFER)	Davide Beretta (EIFER)
1.3	2015/05/30	Second version (EIFER)	Christoph Kaendler (EIFER)
1.3	2015/05/30	Second revision (EIFER)	Davide Beretta (EIFER)
1.3	2015/05/30	Third version (EIFER)	Christoph Kaendler (EIFER)
2.0	2015/05/30	Final version	Christoph Kaendler (EIFER)

# Table of Contents

<b>1</b>	<b>Hybrid prognostics approach based on a behavioral model</b>	<b>5</b>
1.1	Basics of the model . . . . .	5
1.1.1	Recall of the model . . . . .	5
1.1.2	Constraints on the parameters . . . . .	7
1.2	Evaluation of the simulations' performances . . . . .	8
1.3	Data used . . . . .	9
1.4	Prediction and performance evaluation . . . . .	10
1.4.1	Prediction for Exp. 1 . . . . .	10
1.4.2	Prediction for Exp. 2 . . . . .	17
1.4.3	Synthesis of the results . . . . .	23
1.5	Algorithm for the system . . . . .	24
1.5.1	Architecture . . . . .	24
1.5.2	Genericity analysis . . . . .	26
1.6	Conclusion . . . . .	28
<b>2</b>	<b>Multiple model approach</b>	<b>31</b>
2.1	Investigation of the correct detectability for different ageing rates . . . . .	31
2.1.1	Method . . . . .	31
2.1.2	The artificial voltage signal . . . . .	31
2.1.3	Investigation procedure . . . . .	33
2.1.4	The investigation of measurement system constraints . . . . .	34
2.1.5	conclusion . . . . .	38
2.1.6	Impact of ageing rates . . . . .	39
2.1.7	Ageing Rate and Standard Deviation Detection . . . . .	40
2.2	Evaluation of the prognosis . . . . .	42
2.3	Data used . . . . .	42
2.4	Prediction . . . . .	43
2.5	Algorithm for the system . . . . .	43
2.5.1	Architecture . . . . .	43
2.6	Conclusion . . . . .	44



# Chapter 1

## Hybrid prognostics approach based on a behavioral model

### 1.1 Basics of the model

#### 1.1.1 Recall of the model

In this section is presented a quick recall of the model used for the hybrid prognostics approach. More details and a complete description can be found in [1] and D6.1.

The input of this model is the current which is normalized as current density to be decomposed in alternative and continuous parts. These two current densities are the input of the static and dynamic models. The outputs of these models are recomposed in voltage per cell to finally be de normalized in voltage.

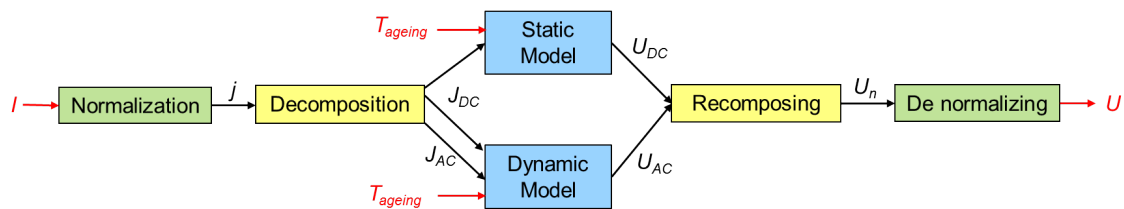


Figure 1.1: Scheme of the model

The aim of the dynamic part of the model is to link voltage variations with the current variation around a static operating point. This part of the model is based on an electrical equivalency. Indeed, the physical phenomena are represented by an impedance (Figure 1.2).

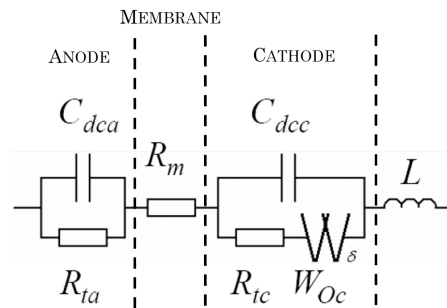


Figure 1.2: Electrical equivalency impedance of the dynamic model

The static part is based on a development of the Butler Volmer law with a difference made between the electrodes (eq. (1.1)) :

$$U_{DC} = E_n - R_m \cdot J_{DC} - \frac{1}{b_a} \cdot \operatorname{asinh} \left( \frac{J_{DC}}{2 \cdot j_{0a}} \right) - \frac{1}{b_c} \cdot \operatorname{asinh} \left( \frac{J_{DC}}{2 \cdot j_{0c} \cdot \left( 1 - \frac{J_{DC}}{j_{Lc}} \right)} \right) \quad (1.1)$$

The time is included in the model (Figure 1.1). The process realized is described on the figure 1.3.

Thanks to a characterization (composed of EISs and one polarization curve), the values of the parameters can be obtained for the time considered (Figure 1.3) with the updating procedure. It is realized on all the characterization learnt. Then exponential models are obtained with an identification thanks to the parameters values.

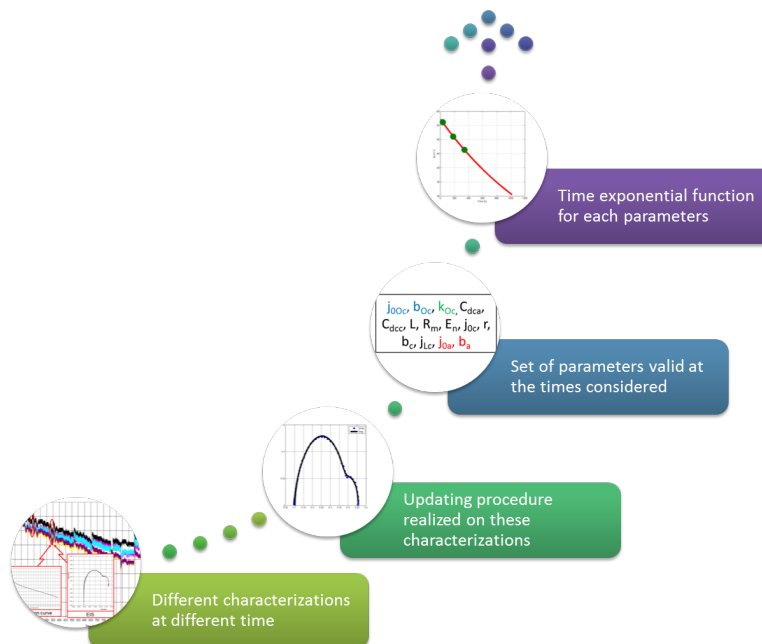
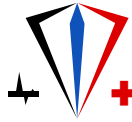


Figure 1.3: Process for initializing the ageing model



The parameters chosen for evolving with the time are modeled by an exponential function (eq. (1.2)).

$$Param(t) = \alpha \cdot e^{\beta \cdot t} \quad (1.2)$$

Both parameters ( $\alpha$ ,  $\beta$ ) are identified by a fitting with of the expression (eq. (1.2)) and the values obtained from the experimentation.

### 1.1.2 Constraints on the parameters

We had to compose with the actual knowledge of the PEMFC's ageing, which were not complete enough. Indeed, the ageing of the physical phenomenon represented by the parameters aren't known well enough for a specific modeling.

On the previous deliverable (D6.1), it was shown that some parameters don't have a clear tendency with the time. It makes the identification of the exponential functions difficult with high error. In order to face this issue, two types of analysis were accomplished.

- A parameters sensibility analysis was realized, it allowed to evaluate the influence of each parameters on the model (developed on the D6.1).
- A statistical analysis was realized: with five set of data (single cell or stack) the updating procedure was realized three different ways. With three different algorithms for the regressions, the updating procedure was done on all the characterizations available on the set of data. Thus, fifteen tendencies were observed for each parameters (increasing, constant or decreasing). The comparison of these tendencies allowed to see if there is a redundancy or not. We considered that when a parameter presents a majority of the same tendency it can be imposed this way.

With these two studies it was possible to make hypothesis on some parameters, and so impose them constant, increasing or decreasing in the algorithm. The choices made are reported on the table 1.1.



Parameter	Choice
$C_{dca}$	Regressed on the first carac. then fixed
$C_{dcc}$	Regressed on the first then fixed
$b_{Oc}$	Free of constraints
$j_{0Oc}$	Regressed on the first then fixed
$k_{Oc}$	Free of constraints
$L$	Regressed on the first then fixed
$R_m$	Free of constraints
$R_{Oc}$	Regressed on the first then imposed increasing
$\tau_{Oc}$	Regressed on the first then imposed increasing
$b_a$	Free of constraints
$j_{0a}$	Regressed on the first then fixed
$b_c$	Regressed on the first then imposed decreasing
$j_{0c}$	Free of constraints
$j_{Lc}$	Regressed on the first then fixed

Table 1.1: Constraints on the parameters' evolutions with time

## 1.2 Evaluation of the simulations' performances

In order to evaluate and compare the simulations, errors' calculations are used. They are defined as described under.

- The RMSE (Root-Mean-Square Error) is a value representing the standard deviation between two values.

$$RMSE = \sqrt{\frac{1}{\text{Number of points}} \cdot \sum_{\text{Points}} (\text{Measure} - \text{Estimation})^2} \quad (1.3)$$

- The MAPE (Mean Absolute Percentage Error) is an error value measuring the precision of an estimation.

$$MAPE = \text{Mean}_{\text{Points}} \left( \left| 100 \cdot \frac{(\text{Measure} - \text{Estimation})}{\text{Measure}} \right| \right) \quad (1.4)$$

- The determination coefficient ( $R^2$ ) is an indicator judging of the quality of a regression. It is between zero and one, with the best option being one, and calibrate the adequacy between the model and the data.

$$R^2 = 1 - \frac{\sum_{\text{Points}} (\text{Measure} - \text{Estimation})^2}{\sum_{\text{Points}} (\text{Measure} - \text{Moyenne}_{\text{Points}}(\text{Measure}))^2} \quad (1.5)$$





## 1.3 Data used

Three set of data are used in the following development. They are described in the following.

- The Exp. 1 is a set of data proposed by FCLAB in the D2.1. This long duration test was realized during around 1000h at FCLAB facilities. The solicitation is a ripple current composed of a DC component of 70A with a triangular dynamic addition (+/ - 10% of 70A at 5kHz). During this experiment, a complete characterization is realized once a week. They are composed of a polarization curve and three EIS at three different operating points (0.70A/cm<sup>2</sup>, 0.45A/cm<sup>2</sup> and 0.2A/cm<sup>2</sup>). The current and the voltage are monitored during the whole test. The fuel cell is a five cell stack with a 100cm<sup>2</sup> active area.
- The Exp. 2 is an experiment realized in the frame of SAPPHIRE by ZSW and lasts 2155h. The mission profile is based on a daily profile for a stationary micro co-generation system (Figure 1.4). The stack used, furnished by ZSW, is a five cell stack with an active area of 100cm<sup>2</sup>. It is called a rainbow stack as the membranes are different between the cells. Face to the hypothesis of the homogeneity of the behavior inside the stack, we will consider each cell independently. A characterization is also realized once a week, it is composed of a polarization curve and three EIS (at 0.15A/cm<sup>2</sup>, 0.25A/cm<sup>2</sup> and 0.35A/cm<sup>2</sup>). The solicitation and the voltages of the cells are also monitored. The two first characterizations cannot be used here as some EIS are missing and it makes the results not comparable.

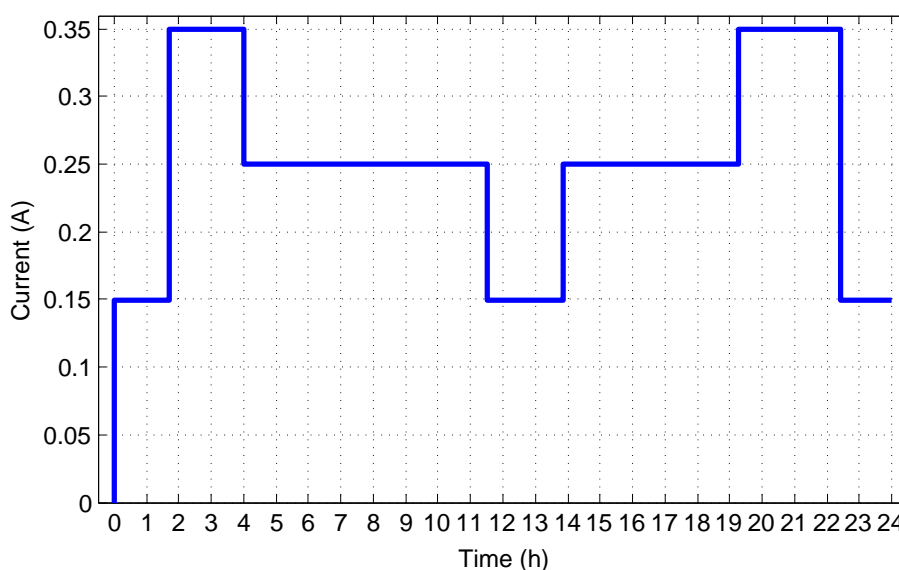


Figure 1.4: Co-generation profile

- The Exp. 3 was realized during SAPPHIRE by FCLAB. On a stack of the same kind as Exp. 2, the experiment lasts 800h. The solicitation is based on the same profile, with the amplitude doubled and 10 cycles per day. Only two characterizations were measured, at the start and at the end of the experiment. It is composed of a polarization curve and 3 EIS at 0.3A/cm<sup>2</sup>, 0.5A/cm<sup>2</sup> and 0.7A/cm<sup>2</sup>.



## 1.4 Prediction and performance evaluation

Tests were performed on the two firsts data set in order to assess the capability of prognostics approaches to estimate the state of health (SoH) of the fuel cell and predict its behavior.

For this evaluation, each set of data is treated as following.

- The updating procedure is realized on all the characterizations available. The quality of it is discussed.
- The necessary learning set is studied then. The main objective being the prediction of the behavior, the errors' results at the end of the prediction is used for comparing the learning set sizes. These errors are more developed in the last study, but used here for choosing the best compromise learning / accuracy. This step allows the choice of the number of characterization learnt.
- Then the identification of the exponential models can be realized based on the values of the parameters obtained with the learning set chosen. The quality of these is evaluated.
- Finally, the quality of the prediction is specified. For this, the prediction of polarization curves and voltage is studied.

### 1.4.1 Prediction for Exp. 1

#### Updating procedure

The updating procedure is realized for all of the characterizations. The parameters are identified in order for the model to fit as best as possible to the characterizations' data. The tables 1.2 and 1.3 reports the mean errors between the model and the data on all the characterizations for the polarization curves and EIS.

	Mean error
RMSE (V)	$4.91E^{-3}$
$R^2$	0.996

Table 1.2: Mean errors on the polarization curve fitting

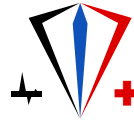
	Imaginary part	Real part
RMSE	$3.09E^{-3}$	$2.74E^{-3}$
$R^2$	0.99	0.9993

Table 1.3: Mean errors of the Nyquist plans' fitting

The model is able to fit the data with a great accuracy.

#### Amount of characterizations to learn

The prediction of the behavior (voltage with ageing) being our principal goal, we are trying to find the best balance between quality of prediction and amount of characterizations learnt.



The ageing of the parameters being modeled by exponential functions with two sub-parameters (eq. (1.2)), the minimum learnt is two characterizations.

Seven simulation are realized, as there are 7 possibilities for the learning set. Indeed, the amount of characterization used (and so learnt) is between 2 and 8.

We are anticipating slightly the study detailed in the section 1.4.1, as the prediction of the voltage allows to compare the results.

The error between the prediction and the measure of the stack's voltage is calculated . It was done at the end of the prediction, so between 900h and 1016h.

The following step are realized for each line of the table 1.4 :

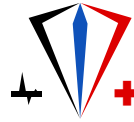
- the available characterizations are listed in the first column;
- the updating procedure are realized on them [1];
- the obtained parameters' values are used in order to realize an identification for the exponential models (eq. (1.2));
- these functions are used in the global model (Figures 1.1 and 1.3);
- the global model is simulated under the solicitation measured during the experiment;
- the errors at the end of the test (between 900h and 1016h) are calculated and reported on the last columns.

Characterizations learnt	MAPE (%)	RMSE (V)
0h et 35h (2)	21,9	0.68
0h, 35h et 182h (3)	.92	0.03
0h, 35h, 182h et 343h (4)	0.96	0.03
0h, 35h, 182h, 343h et 515h (5)	0.96	0.03
0h, 35h, 182h, 343h, 515h et 666h (6)	1	0.03
0h, 35h, 182h, 343h, 515h, 666h et 830h (7)	1.3	0.04
0h, 35h, 182h, 343h, 515h, 666h, 830h et 1016h (8)	1.3	0.04

Table 1.4: Errors between the simulated and measured voltage between 900h and 1016h

The table 1.4 allows comparing the quality of the prediction depending of the learning, and so to analyze the improvement brought by the increase of the learning set. The more precise description of the quality of the prediction is done later on the section 1.4.1. Indeed, it is not possible to describe the results of each test, we choose to present only the option with the best compromise size of learning set / quality of the voltage's prediction.

The evolution of the errors with the increasing of the learning set size is surprising. We could have expected the error to decrease with the increase of the learning set. However, it is not that simple on this data set. With only two characterizations, the results are catastrophic, it is logical as any error on the measures or on the regressions have a direct impact.



When three characterizations are used, the results present the minimal errors. With more than four used, the errors obtained are almost stable. Up to six, the prediction's quality decrease. However, with more than three characterizations learnt, the errors' variations are finally low.

If a brutal change on the ageing of the stack would have happened, adding characterizations would bring the change needed in the exponential models.

In the end, we can use only three characterizations for the prediction of the Exp. 1 described in the following.

## Exponential functions identification

The direct implication of the chosen amount of characterizations learnt is the identification of the exponential functions. This part is not a major concern, but it can still be interesting.

The values of the fixed parameters are reported in the table 1.5.

Parameters	Obtained values
$C_{dca}$	0.033 [F/cm <sup>2</sup> ]
$C_{dcc}$	0.032 [F/cm <sup>2</sup> ]
$E_n$	1 [V]
$j_{0a}$	0.271 [A/cm <sup>2</sup> ]
$j_{0Oc}$	0.25 [A/cm <sup>2</sup> ]
$j_{Lc}$	1.78 [A/cm <sup>2</sup> ]
$L$	$1.65E^{-6}$ [H.cm <sup>2</sup> ]

Table 1.5: Fixed parameters' values

The values of the other parameters obtained at 0h, 35h and 182h are used for the exponential models identifications. Starting this last time, the global model works without considering any other data.

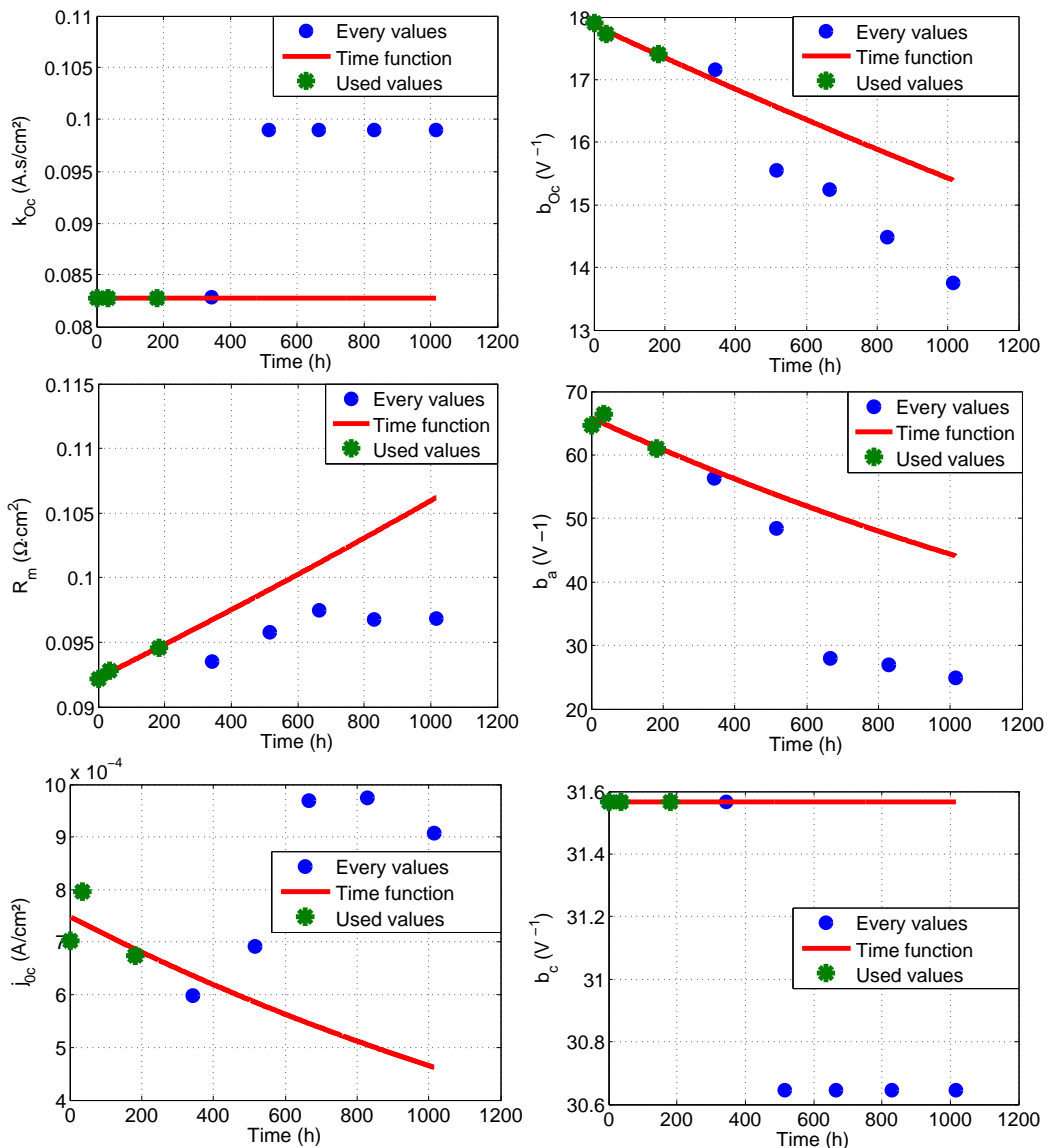
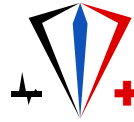
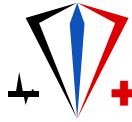


Figure 1.5: Evolution of the parameters with the exponential function obtained on the three first values for Exp. 1

Even though we are only using three characterizations, the complete set of data is known. We can then compare the estimations of the parameters with the values obtained at the updating procedure step. For the parameters' values we talk about "estimation" as the values, on which the functions are based, are not a measurement but already an estimation.

The figure 1.5 shows the obtained functions for the parameters as well as all the points.

Mainly, the tendencies of the time functions are coherent with the values. For  $b_{Oc}$ , the tendency is followed but the estimation is slightly different; as well as for  $b_a$  and  $R_m$ . For some others, the estimations are further from the first values.  $b_c$  and  $k_{Oc}$  present a step that cannot be anticipated with the amount of data taken into account. These two parameters seems however to compensate each other. The cathodic exchange current density hasn't a clear evolution with the time.



Parameter	MAPE (%)
$b_{Oc}$	4.4
$k_{Oc}$	8.6
$R_m$	3.4
$b_a$	31.5
$b_c$	1.5
$j_{0c}$	22

Table 1.6: MAPE calculated between the parametric values obtained at the updating procedure and the ones obtained with the exponential functions

A certain gap is exposed between the estimation of the values with the exponential functions and with the updating procedure (Table 1.6).

The identification of the parameters' models is done thanks to values. However, these values are not for sure the real values that each parameter have during the experiment. Indeed, the results on the updating procedure can be a mathematical solution with a loss of the physical meaning.

The proposed approach being hybrid, this divergence is not an issue. Indeed, the true concern is the following part: the prediction of the behavior.

## Behavior prediction

The characterizations learnt are still the three firsts. Here our goal is the validate the prediction abilities of the proposed approach.

The error between the measure and the simulation of the voltage at the end of the prediction (between 900h and 1016h), is 0.92% (MAPE) and 0.03V (RMSE) (Table 1.4) : a very good result. This can be confirmed by a look at the figure 1.6. On this figure, we can see the output of the model and the real stack under the same solicitation at the period of this calculation (between 900h and 1016h).

The behavior prediction is very satisfying on this end of the experiment. In the traditional consideration of the RUL's prediction, the tolerance on the prediction's error is lowering with the time. Thus, a good prediction at the end of the simulation is very important.

With less than a percent of error at the end of the prediction, the prediction, presented on figure 1.7, is completely accurate with the errors being 1.05% (MAPE) and 0.08V (RMSE) on the totality.

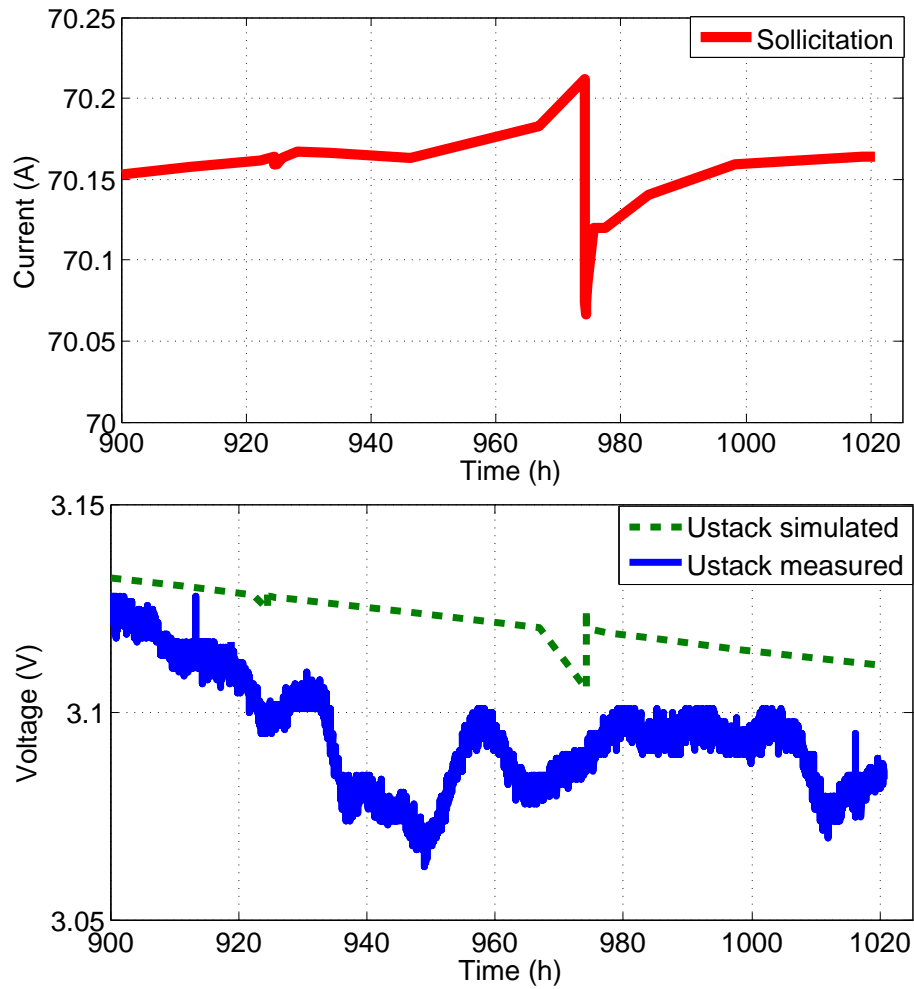


Figure 1.6: Prediction (with 3 characterizations learnt) and measure at the end of the experiment

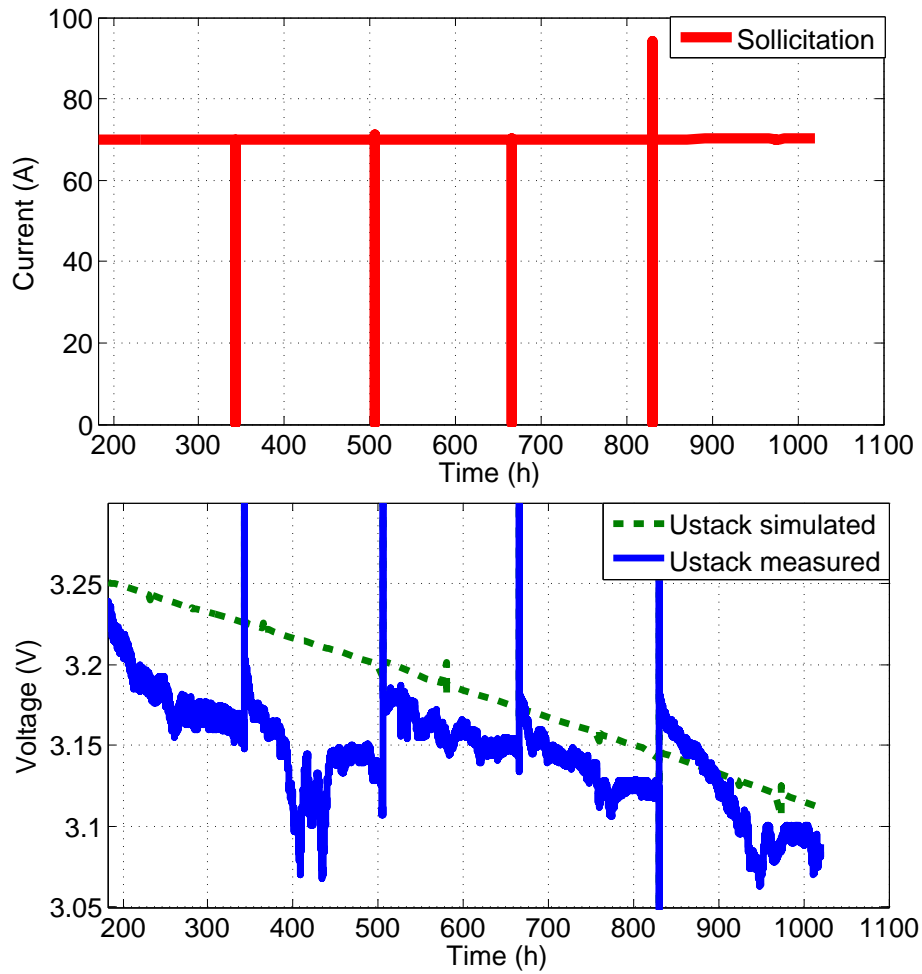
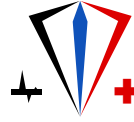


Figure 1.7: Prediction and measure on the complete simulation (starts at 182h as it is the time when the prediction starts)

With the static model, we are able to compare the prediction of polarization curves with the measured ones. The figure 1.8 presents this comparison at the eighth one.



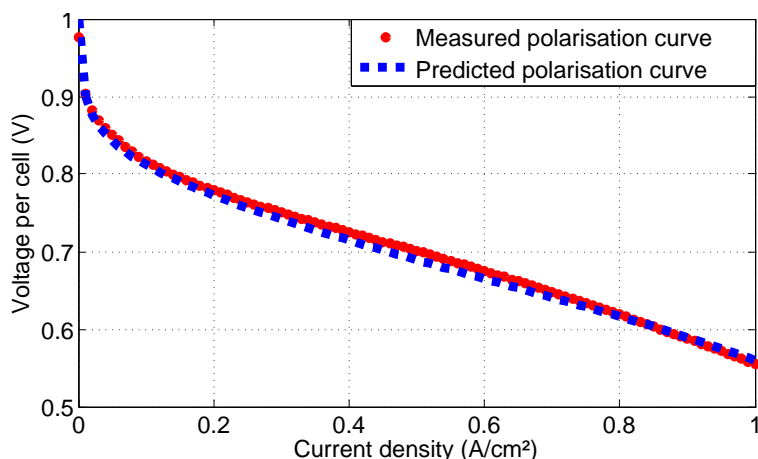
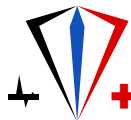


Figure 1.8: Prediction of the eighth polarization curve 1016h

Courbe de polarisation	MAPE (%)	$R^2$
4 (343h)	0.25	0.998
5 (515h)	0.3	0.999
6 (666h)	0.35	0.999
7 (830h)	0.76	0.995
8 (1016h)	0.99	0.992

Table 1.7: Error between the measured and simulated(i.e. predicted) polarization curves

For all the polarization curves available, the prediction is accurate (Tableau 1.7). For the fourth, at 343h, the MAPE error is 0.25% with an adjustment coefficient of 0.998. For the last one, at 1016h, the MAPE error is 0.99% with an adjustment coefficient of 0.992.

Even though the errors on the predictions grow with the time, their values are still demonstrating an accurate prediction with an adjustment coefficient included between 0.99 and 1.

Finally the use of the model for the prediction with this set of data is particularly satisfying. The mean error on the total prediction is around 1% and even lower at the end. The learning set is composed of only three characterizations. The prediction starts at 182h for a prediction of around 1000h. So even though the data used are more consequent, the prediction can be started really early.

## 1.4.2 Prediction for Exp. 2

The use of only one set of data is not enough for demonstrating the ability of the approach to predict the behavior. Thus we propose the same analysis that was presented for the Exp. 1 to the Exp. 2.

In the following, are evaluated in order:

- the quality of the updating procedure realized on the usable characterizations;



- the amount of characterizations for the best compromise prediction / learning;
- the estimation of the parameters with the exponential functions;
- the quality of the behavior's and polarization curves' predictions.

The two experiment are completely different, from the stack, the sollicitations, and laboratory. This would allow to confirm that the approach is robust and efficient.

### Updating procedure

Here we are trying to validate the accuracy of the updating procedure. This procedure allows to determine a value for each parameters at a precise time, with a characterization.

On the Exp. 2, the two first characterizations are not homogeneous; for the first one, the polarization curve is missing and for the second, the EIS at  $0.15A/cm^2$ . This issue prevents us from realizing the updating procedure on one hand, and on other hand, as the characterization is not the same, the perturbations it induces are not comparable.

The first characterization we can use is the one  $620h$ . The following are realized at  $800h$ ,  $984h$ ,  $1130h$ ,  $1298h$ ,  $1465h$ ,  $1635h$ ,  $1800h$ ,  $1968h$  and  $2010h$ .

The updating procedure is then realized on all these characterizations. The regressions are realized and their mean errors are reported on tables 1.8 for the polarization curves and 1.9 for the EIS. These errors expose good results. However, in order to be able to have a good fitting, we had to lift the constraint on  $\tau_{Oc}$ . We can then make the hypothesis than this parameter represent a phenomenon that can make it increase and decrease with the ageing time in a non monotonic way..

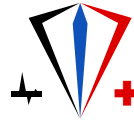
	Mean error
RMSE	$2.25E^{-2}$
$R^2$	0.986

Table 1.8: Mean errors obtained on the polarization curves' regressions (except the first two)

	Imaginary part	Real part
RMSE	$4,82E^{-3}$	$3,17E^{-3}$
$R^2$	0.989	0.9995

Table 1.9: Mean errors on the Nyquist plans' regressions for the imaginary and real parts (except the first two)

The updating procedure allows again to have a good fitting between the data and the simulations.



## Amount of characterizations to learn

The exponential models are identified with the amount of characterizations considered. They are then used for defining the time evolution of the parameters in order to simulate the global model. The error between the simulation and the measurement is used for comparison but studied more extensively in the section 1.4.2.

The table 1.10 presents the results of the error at the end of the experiment in function of the number of characterization learnt.

Characterizations learnt	MAPE (%)	RMSE
2 (620h and 800h)	6.6	0.057
3 (... and 984h)	3.9	0.037
4 (... and 1130h)	4.4	0.039
5 (... and 1298h)	3.9	0.037
6 (... and 1465h)	3.9	0.038
7 (... and 1635h)	4.1	0.039
8 (... and 1800h)	3.9	0.038
9 (... and 1968h)	4	0.038
10 (... and 2010h)	4	0.038

Table 1.10: Error on the voltage prediction at the end of the simulation (between 2000h and 2120h)

The errors don't change a lot, and no clear tendency appears. It is however clear that only two characterizations are not enough for the identification of the exponential models.

For this experiment, the amount of characterizations bringing the best compromise is three. It is finally the same conclusion than for the Exp. 1: we can suppose that three characterizations will be enough for a good prediction.

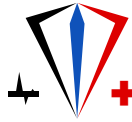
For the following, three characterizations are used for the learning set.

## Exponential functions identification

The parametric values obtained are used for the identification of the exponential models. They will be used in the global model as the time evolution of the parameters.

Only three characterizations are used for the learning phase but the other are still available and allow to compare with the simulations results.

The parameters's estimation shows the same features as earlier. For the majority of them, the tendency is coherent but with different values (Figure 1.9). Indeed, as we can see in the table 1.11, the error between the estimations of the parametric values obtained with the exponential functions and with the updating procedure can be qualified as considerable.



Parameters	MAPE (%)
$b_{Oc}$	31
$k_{Oc}$	79
$R_m$	18
$b_a$	5.8
$b_c$	3.7
$j_{0c}$	42

Table 1.11: MAPE errors calculated between the parametric values estimations for the regression and the estimation

The exchange current density at the cathode  $j_{0c}$  is one more time the parameter the most difficult to fit. Its tendency goes the other way at the half of the experiment, it cannot be anticipated.

The table 1.12 report the values of the fixed parameters. They are finally close to the ones obtained with Exp. 1. However,  $j_{0a}$  and  $j_{0Oc}$  are inferior here, it is balanced with  $b_{Oc}$  and  $b_a$  that are superior.

Parameter	Values obtained
$C_{dca}$	0.036 [F/cm <sup>2</sup> ]
$C_{dcc}$	0.022 [F/cm <sup>2</sup> ]
$E_n$	1 [V]
$j_{0a}$	0.042 [A/cm <sup>2</sup> ]
$j_{0Oc}$	$1.E^{-8}$ [A/cm <sup>2</sup> ]
$j_{Lc}$	1.16 [A/cm <sup>2</sup> ]
$L$	$3.29E^{-7}$ [H.cm <sup>2</sup> ]

Table 1.12: Fixed parameters' values

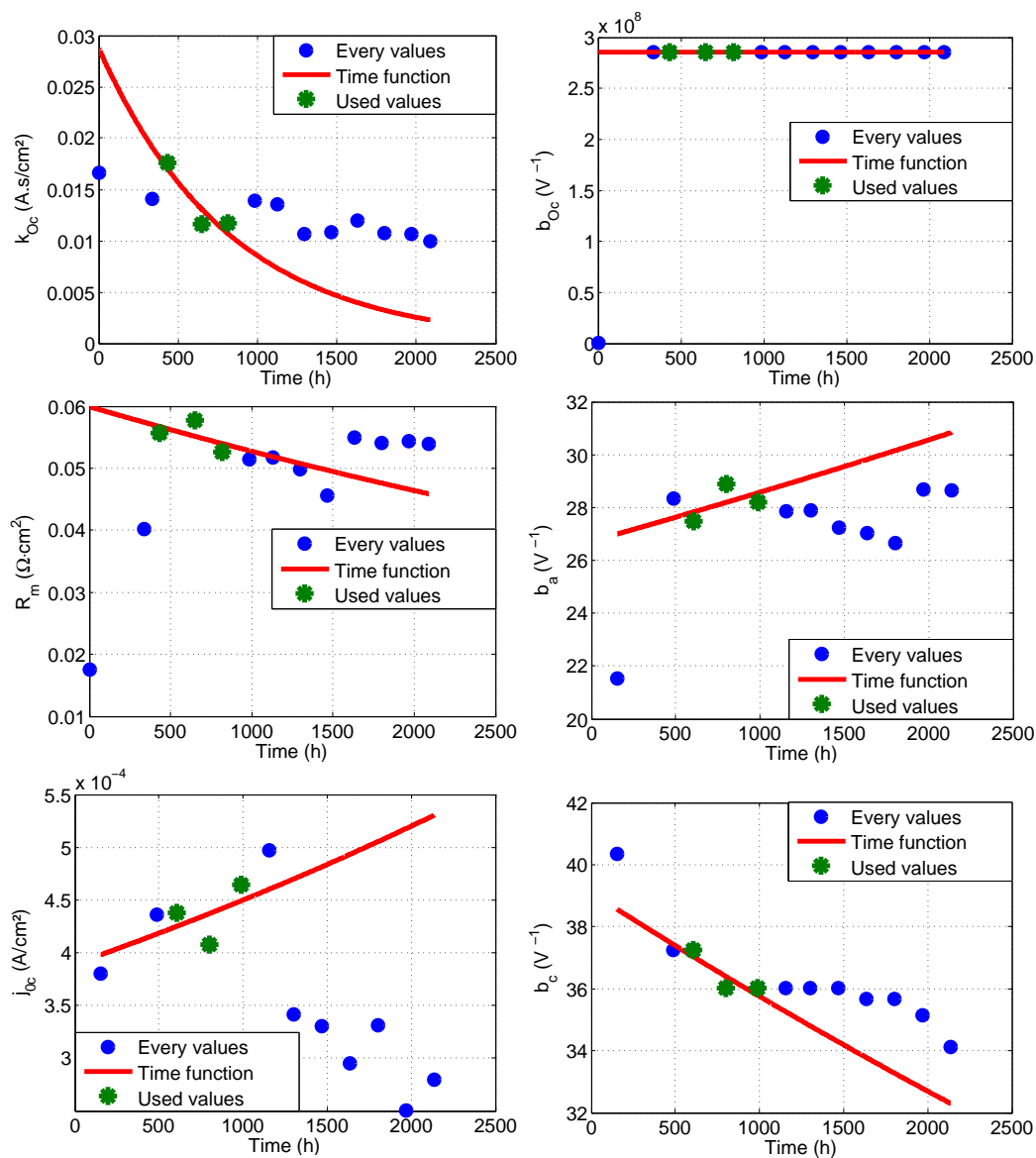
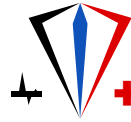


Figure 1.9: Time evolution with the exponential fitting for the Exp. 2

## Behavior prediction

The exponential functions presented on the last section are used in the global model. They represent the evolution of the parameters' values with the time.

Expose the results on a figure is not easy. Indeed, the solicitation is a cycle per 24h and the prediction is realized for 1100h. As the prediction starts after the last characterization used that happened at 984h. So it is not possible to present a figure with the complete prediction.

The figure 1.10 offers the plot of the simulation and the measure at the end of the prediction.

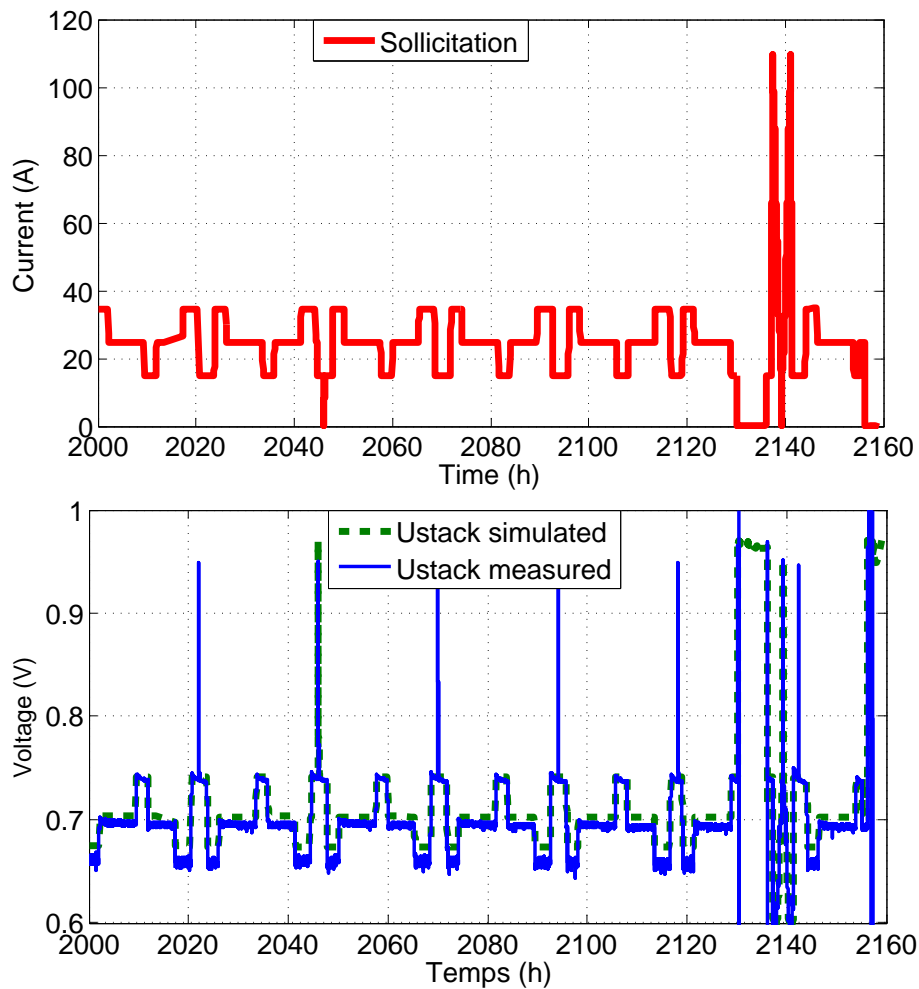


Figure 1.10: Measure and prediction at the end of the prediction (between 2000h and 2160h)

As we can see, the cell's voltage was measured as zero for some points. It prevents us from calculating the MAPE error on the complete prediction which has a RMSE of 0.12V. The calculation of the error was realized at the end of the prediction, between 2000h and 2120h in order to avoid the zeros. The MAPE on this period is 3.9% and the RMSE is 0.037V.

The estimation of the polarization curves is also satisfying, as it can be seen of the figure 1.11.

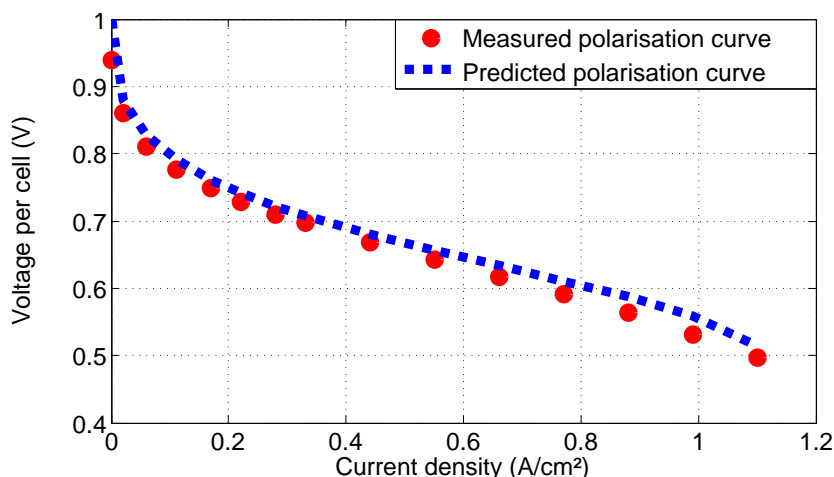
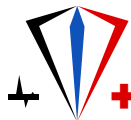


Figure 1.11: Prediction of the 12<sup>th</sup> polarization curve (at 2010h)

Polarization curve	MAPE (%)	$R^2$
6 (1130h)	1.26	0.98
7 (1298h)	1.12	0.98
8 (1465h)	1.17	0.984
9 (1635h)	1.53	0.983
10 (1800h)	1.69	0.982
11 (1968h)	2.39	0.97
12 (2010h)	2.8	0.96

Table 1.13: Error between the measured and predicted polarization curves

The prediction of the polarization curves is slightly deteriorating with the time, as the MAPE is slightly increasing (Tableau 1.13). These errors are however very low and very honorable.

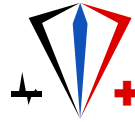
The use of the Exp. 2 confirms that the prediction model is good. With a learning set of only three characterizations, the behavior prediction is very satisfying on the complete experiment.

### 1.4.3 Synthesis of the results

The model has been used for a behavior prediction on two different set of data, obtained on two different stacks, two different test benches, with different solicitations. The Exp. 1 is realized under a ripple current at FCLAB and the Exp. 2 with a cycled solicitation at ZSW.

The learning set chosen in both cases is composed of three characterizations for a prediction of a thousand of hours. It can be considered as a major asset as for the Exp. 1 the prediction is possible after 182h only, and for Exp. 2 after 364h. Even though the amount of data for each characterization is quite important, there is no need for a constant monitoring for a good prediction. The characterizations realized and used for the learning set have to let appear some ageing.

The table 1.14 reports the synthesis of the errors' calculations realized previously:



- for the voltage prediction:
  - for the Exp. 1 between 900h and 1016h;
  - for the Exp. 2 between 2000h and 2120h;
- for the prediction of the last polarization curve :
  - for the Exp. 1 the 8<sup>th</sup>;
  - for the Exp. 2 the 12<sup>th</sup>.

	Learning set	Pola. predictions	Final behavior's predictions
Exp. 1	182h	0.99%	0.92%
Exp. 2	364h	2.8%	3.9%

Table 1.14: MAPE on the predictions

The prognostics approach appears to give very good results. Nevertheless (and obviously), best performances are obtained in the case of simplest mission profile (experiment 1). As for computational complexity is concerned, note also that the simulation time for the characterization treatment is less than 5 minutes for the first experiment and a bit more than 3 minutes for the following. Also, the simulation allowing the prediction of the voltage takes 2.2 seconds for 1000 hours is Exp. 1. Computation time is therefore low compared to the range of the prediction (PC with 4Go of RAM and a processor of 3.20GHz).

## 1.5 Algorithm for the system

The proposed prognostics approach is proven as accurate and efficient. The scientific issue is treated, we now can consider the implementation issue.

### 1.5.1 Architecture

Thanks to an intern, Aiman Arshad, the algorithm was transferred on Labview. The architecture chosen is optimized for the user and composed of four "projects" (Lview vocabulary).

These four projects allows the user to realize the majority of the needed steps for the good use of the model. Indeed, a part is not treated here, the EIS; as the system is not yet equipped for this measurement.

- The first project aims at estimating the stack's voltage. The inputs are the current evolution and the time as well as the exponential parameters and the stack characteristics. This project is simply the transcripts of the global model.



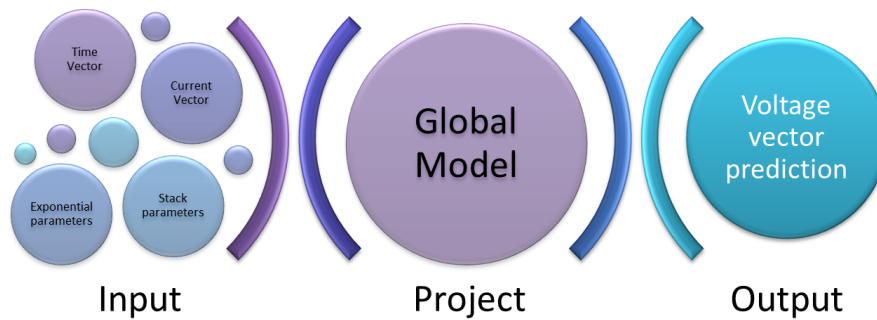


Figure 1.12: First project synoptic

- The second project aims at estimate a polarization curve with the static model only. For this goal, the inputs are the currents points and the values of the static parameters.

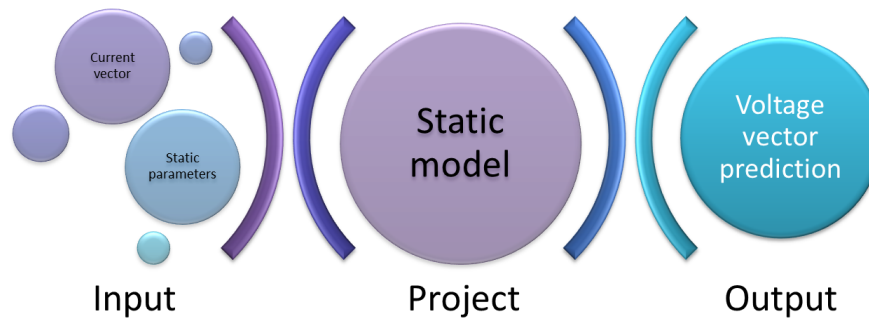


Figure 1.13: Second project synoptic

- The third project is the updating procedure. Thanks to a polarization curve, the updating procedure of the static model is done. When three or more curves have been treated, the exponential parameters are identified.

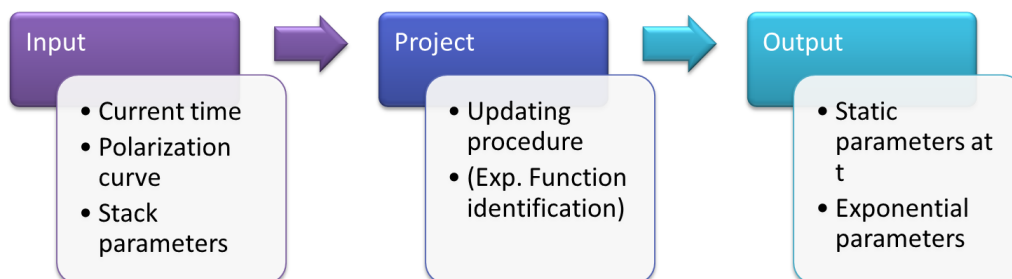


Figure 1.14: Third project synoptic

- The last project is the first one with an add-on. The frame of the remaining useful life is furnished. Under a constant sollicitation of  $0.35A/cm^2$  the voltage output is studied in

order to know when it is lower than the threshold: 27,4V. The output of this project is the time at which the threshold is overtaken, and the last computation time on which the threshold was no hit yet. A frame for the RUL is then furnished.

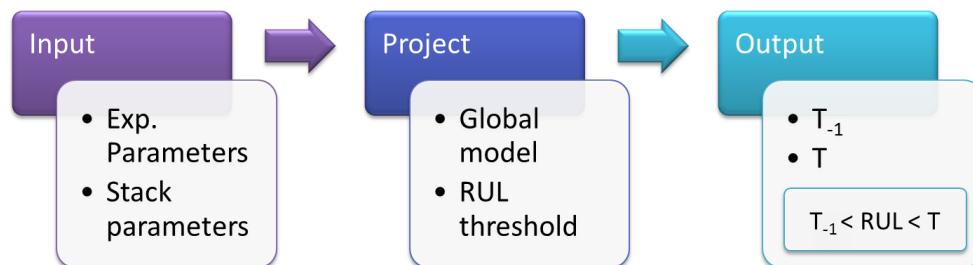


Figure 1.15: Synoptique du quatrième projet

The main limit here is the EIS's measurement impossibility . However, an other European project, D-CODE [2] aims at elaborating a system for EIS measurement at low costs and low dimensions. The use of impedance measurements is compatible with an online implementation. Meanwhile, the absence of impedance measures must be compensated.

## 1.5.2 Genericity analysis

### Problematic and suggestion

On the dynamic side, the parameters cannot be obtained: without EIS we cannot realize the updating procedure on the dynamic model. The suggestion we offer is to use another set of data for the prediction. The accuracy of the prognostics approach is assessed by considering that exponential parameters can be obtained by using an other dataset. In order to validate or invalidate this possibility, simulations are realized.

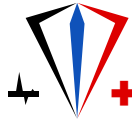
A strength of the approach proposed is its adaptability at different stacks. However, the hypothesis we make with this suggestion is a strong one: the ageing of similar stacks under similar solicitations are similar.

### Validation

In order to confirm if it is possible to combine the measures and results of two different stacks, the updating procedure is realized on the Exp. 3. The parametric values allow to set the first exponential sub-parameter. Indeed, it is the value taken by the parameter at the time 0. The second sub-parameter is fixed using the values obtained for the Exp. 2 (Section 1.4.2).

So, we propose to:

1. realize the updating procedure on the characterization at the time 0 for the Exp. 3;
2. realize the updating procedure and the exponential functions' identification for the Exp. 2;



3. create the exponential model for the Exp. 3: in the equation (1.2) that represents the time evolution of the parameters, fix the  $\alpha$  with the 1. and the 2. allows to fix the  $\beta$ .

For the first point, the fitting of the model with the data gives good results (Table 1.15). One more time, the adjustment coefficients are very close to 1.

	Pola	(EIS) Imaginary part	(EIS) Real part
RMSE	$7.84E^{-3}$	$1.11E^{-2}$	$1.26E^{-2}$
$R^2$	0.993	0.961	0.995

Table 1.15: Errors obtained on the updating procedure on the first characterization (Mean for the EIS)

The quality of the prediction is evaluated on the last 200 hours. On the same way as earlier, showing the totality of the simulation on one figure is not possible because of the cycles. The figure 1.16 shows a small portion at the end of the prediction.

With the protocol presented, the voltage's prediction of the error between 600h and 800h is 3.03% for the MAPE, 0.025V for the RMSE with an adjustment coefficient at 0.92. These results are very satisfying.

The experiments' cycles being 10 per day the figure 1.16 shows only a short period of time that doesn't let see any ageing. However, the calculation of errors allows to demonstrate the satisfaction of the prediction.

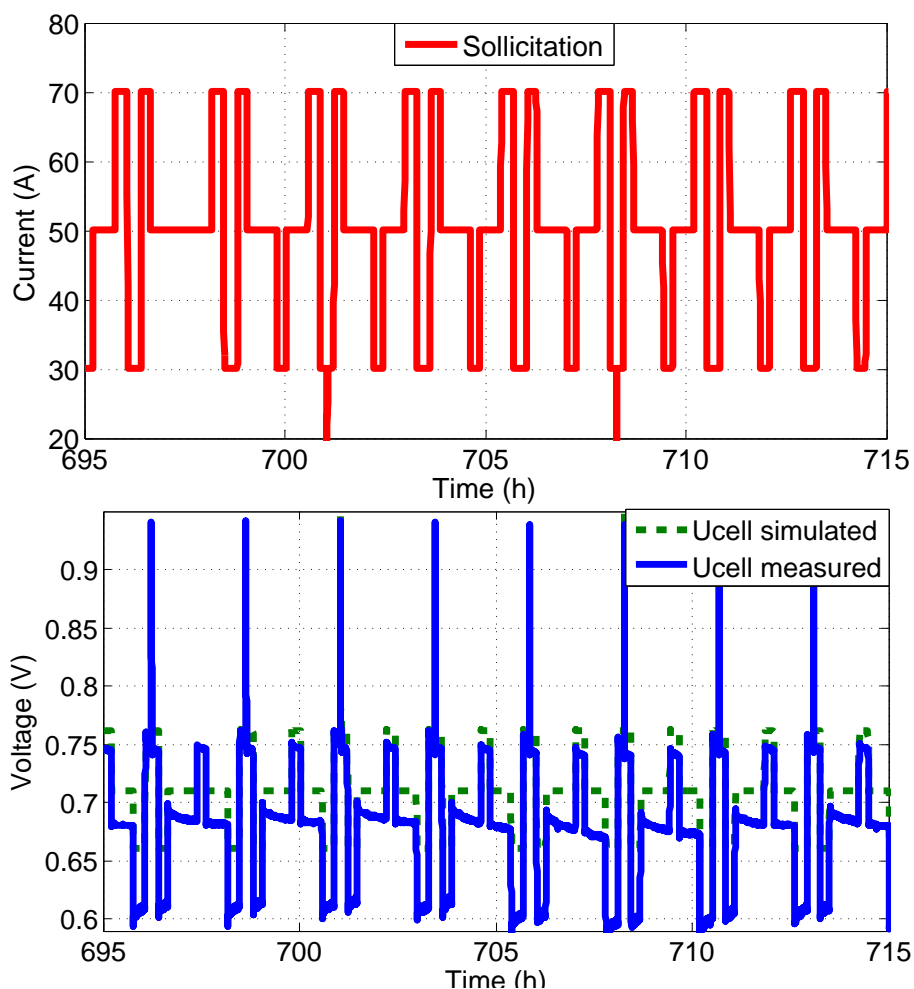
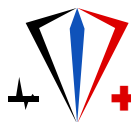


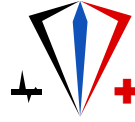
Figure 1.16: Prediction and measure at the end of the test

Finally, it is possible to combine an initial characterization with the study of an other set of data in order to obtain a good prediction. The hypothesis done for the online implementation is coherent.

## 1.6 Conclusion

The proposed approach is able to propose a good prediction with a short amount of time. Indeed, for the Exp. 1, three characterizations represent only 182h. However, the characterizations taken for the learning set, have to let ageing appear, this means that these three characterizations have to be carried out along a sufficient duration, once a week as in the laboratory experiments used for the validation for instance.. On the two data sets, the errors on the prediction of the polarization curve is under 3% and for the behavior at the end, under 4%.

The implementation on a system is presented, with its hypothesis and architecture. The hypothesis we had to make because of the lack of EIS is validated. However, this hypothesis is really strong, and on the deliverable 2.6 it is proven that thanks to an other european project



[2], and a huge reduction of measured points, that an impedance for this approach can be measured in less than a minute.

The global approach is validated and its use for a real industrial system is not only demonstrated possible, but also realized is a shorter version.



# Chapter 2

## Multiple model approach

The patent has not been submitted yet. In the development of the algorithm, an intermediate step was the investigation of the ageing rate through a general constraint for detecting the ageing rate correctly, which is not part of the patent.

### 2.1 Investigation of the correct detectability for different ageing rates

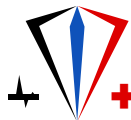
An important parameter for a prognosis algorithm is the decreasing voltage over time. The so-called ageing rate. It determines, how fast the fuel cell ages and when the End of Life (EoL) is reached. A lower ageing rate means a longer life and is a favorable goal to achieve. In addition, in a well optimized system the ageing rate is a long term effect. Unfortunately, it is also very difficult to detect in measured data. The following investigation has been done to estimate the effects of measurement resolution, Signal-to-Noise-Ratio (SNR) and average values on the correct detection of different ageing rates.

#### 2.1.1 Method

In order to isolate the correct ageing rate, different artificial voltages were generated. The benefit of this approach is that the artificial voltage is well-known and the artificial ageing effect is the only effect inside the artificial voltage. For that reason, it is possible to investigate systematically the influence of the measurement device, and of the system constraints on the correct detection of the ageing rate. All the generated voltages have a sampling rate of one sample per second, which was also the acquisition rate of the measurement devices used during the project.

#### 2.1.2 The artificial voltage signal

The goal was to build a constant decreasing voltage with different ageing rates, starting from 7 V (stack) or 0.7 V (cell) and decreasing for 300 hours. After the generation of such a voltage, the Matlab function “awgn” was used to add a Gaussian noise with a SNR of 60 dB, 75 dB or 90 dB to the artificial voltage. The next step was to round the noisy, artificial voltage to 1 mV, 0.1 mV



or 0.01 mV voltage steps in order to create artificial data with different voltage resolutions. The procedure was done for ageing rates of 1, 2, 5 nV/s, 10 nV/s, 20 nV/s, 50 nV/s, 100 nV/s, 200 nV/s, 500 nV/s and 1000 nV/s. Figure 2.1 and Figure 2.2 give a brief overview about the created signals.

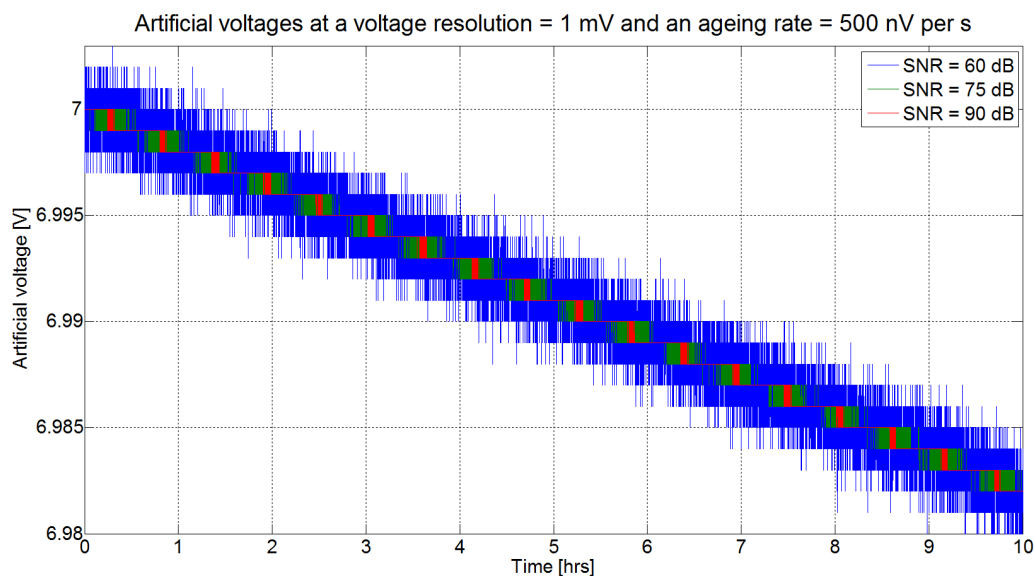


Figure 2.1: An artificially generated voltage for different SNRs.

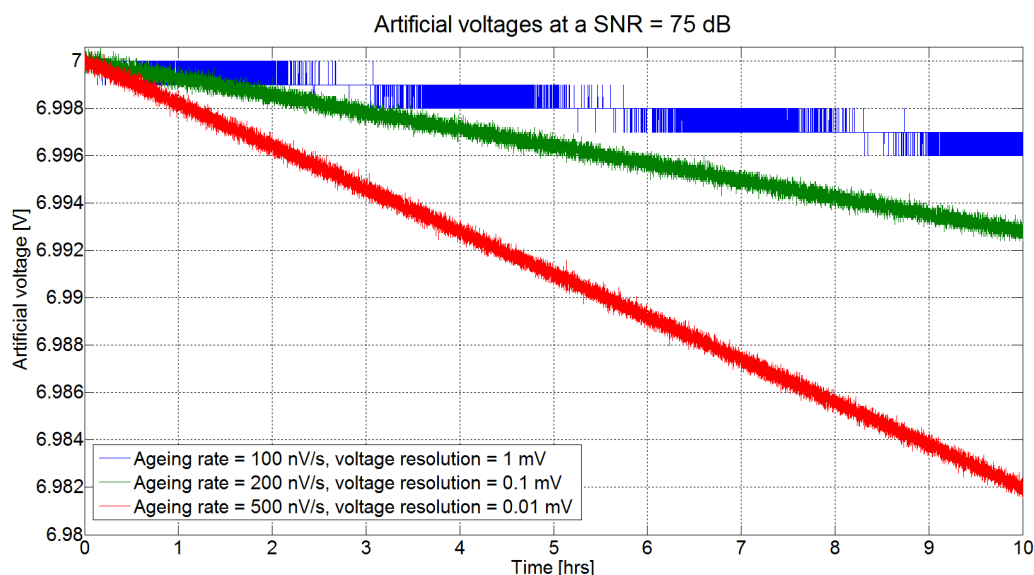
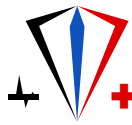


Figure 2.2: Artificially generated voltages for different ageing rates and voltage resolutions.

Figure 2.1 shows the decrease of the voltage during the first 10 hours for an ageing rate of 500 nV/s and different SNRs. An interesting effect is caused by the voltage resolution and an increasing SNR. The high SNR causes remarkable plateaus of voltage, which overlap the ageing





rate. In some intervals, the voltage stays at a constant value, even it is decreasing in the overall trend. As mentioned above, all generated voltages have the same, basic voltage trend and this effect is only caused by the discrete voltage steps of  $1\text{ mV}$  and a high SNR of  $90\text{ dB}$ .

Figure 2.2 shows the voltage decrease over the first 10 hours for voltage resolutions of  $1\text{ mV}$ ,  $0.1\text{ mV}$ ,  $0.01\text{ mV}$  and ageing rates of  $100\text{ nV/s}$ ,  $200\text{ nV/s}$ ,  $500\text{ nV/s}$  at  $75\text{ dB}$  SNR. The low voltage resolution of  $1\text{ mV}$  and  $100\text{ nV/s}$  form again voltage plateaus in some intervals. The two other artificial voltages with an ageing rate of  $200\text{ nV/s}$ ,  $0.1\text{ mV}$  voltage resolution at SNR of  $75\text{ dB}$  and an ageing rate of  $500\text{ nV/s}$ ,  $0.01\text{ mV}$  voltage resolution at SNR of  $75\text{ dB}$ , do not form such plateaus.

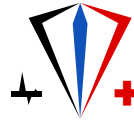
### 2.1.3 Investigation procedure

The general solution to investigate slow, almost linear changing trends is a linear fit inside a determined time interval. As a result, the gradient of the fit represents the ageing rate of a fuel cell voltage. A perfect signal would provide the correct ageing rate directly, but usually, the requested information lies under uncertainties, which are mainly caused by noise, discretization and other measurement impacts.

Applying a linear fit with the least square method to data on a determined time interval gives the average, linear change over time. The size of the time interval/window plays an important role, because a wider time interval means an improved average gradient and decreases the effects of noise and discretization. Unfortunately, a wider time interval increases overall measurement time. In some cases, this additional time is not available. In order to find the correct ageing rate for a fuel cell, it has to be run at steady state for that time interval. For that reason, the artificial voltage was investigated for different time windows. In addition, 100 positions inside the artificial voltage were picked randomly and at these positions the different time windows were investigated. In addition, 100 positions inside the artificial voltage were picked randomly and at these positions the decided time windows were investigated. The first approach has been finding the maximum relative error within these 100 positions to obtain the worst estimation. The second approach is based on the calculation of an average between the results of all 100 positions and form a mean relative error for each time interval. The results of this investigation are presented in the next section. It is important to highlight that the linear fit is already an averaged estimation of the ageing rate. Using several estimations improves the obtained result. The most unfavorable result is still interesting, because it allows to get a deeper understanding of the worst result which can be obtained by a single time interval. The relative error has been used as representative error to form a more meaningful and understandable comparison between different ageing rates. In addition, using an aging rate with a relative error for a prognosis estimation causes an increasing error propagation over the estimated horizon.

### 2.1.4 The investigation of measurement system constraints

Figure 2.3 is an overview of all maximum relative errors, which is presented in percentage related to the time window of the interval. Especially small ageing rates can cause very big rel-



ative errors for small windows size. Figure 2.4 shows a zoomed part of Figure 2.3, where the maximum relative error is limited to 20% of the correct ageing rate. Both figures represent the result for artificial voltages at  $1\text{ mV}$  voltage resolution and SNR at  $75\text{ dB}$ , which is considered as the standard measurement quality of the equipment used during the project. Figure 2.4 shows that it is even difficult for higher ageing rates (e.g.  $100\text{ nV/s}$ ) to reach a maximal relative error below 2% within a 5.5 hours time window. For smaller ageing rates, the highest relative error is out of the scope. Remarkable is that the error seems to change systematic. This phenomena is related to the discretization and will be explained later.

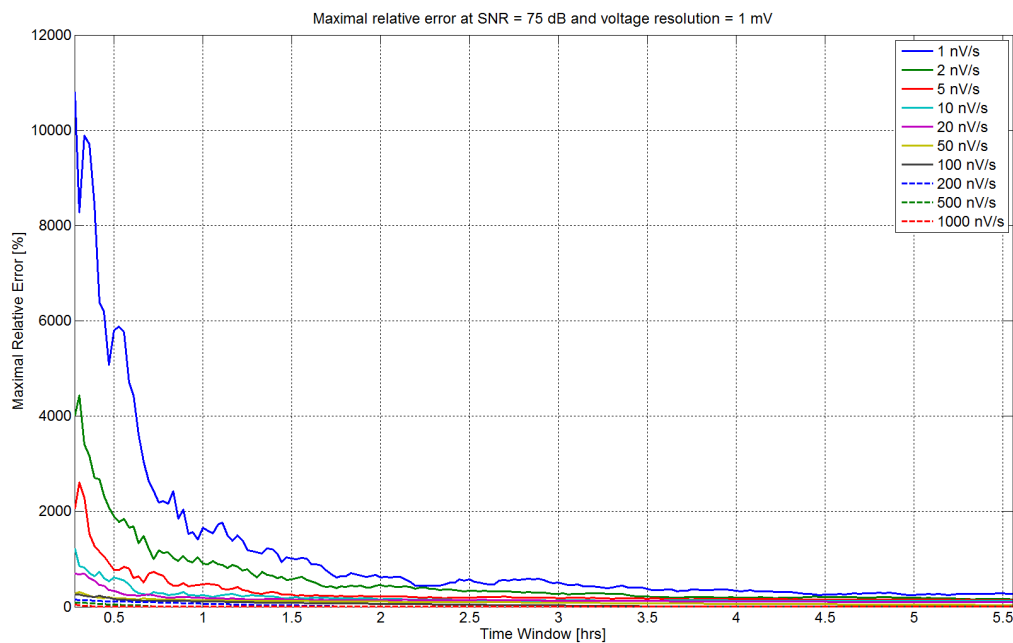
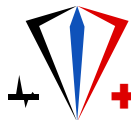


Figure 2.3: Overview of the maximum relative error.

Figure 2.5 presents the mean, relative error in percentage related to the time window size (in hours), zooming the same part of Figure 2.4, it shows the effect of a more average ageing rate. Every ageing rate can be found with a relative error below 10% within a 3 hours time window. In addition, the mean relative error is more random, which is caused by the decision for random positions.

Only at high ageing rates ( $50\text{ nV/s}$  or more) the mean relative error behaves in a comparable and systematic way as the maximum relative error. Taking a closer look to ageing rate of  $20\text{ nV/s}$  it seems to be a transition between the random, noise behavior of the mean relative error and its systematic behavior.

Figure 2.6, Figure 2.7 and Figure 2.8 show on the left side a test or voltage signal with an ageing rate of  $500\text{ nV/s}$  at different SNRs and voltage resolution related to the time. The left window does not show the complete signal and gives only an impression of the used signal to obtain the results on the right side. The right side of these plots represent different results,



based on the voltages on the left side.

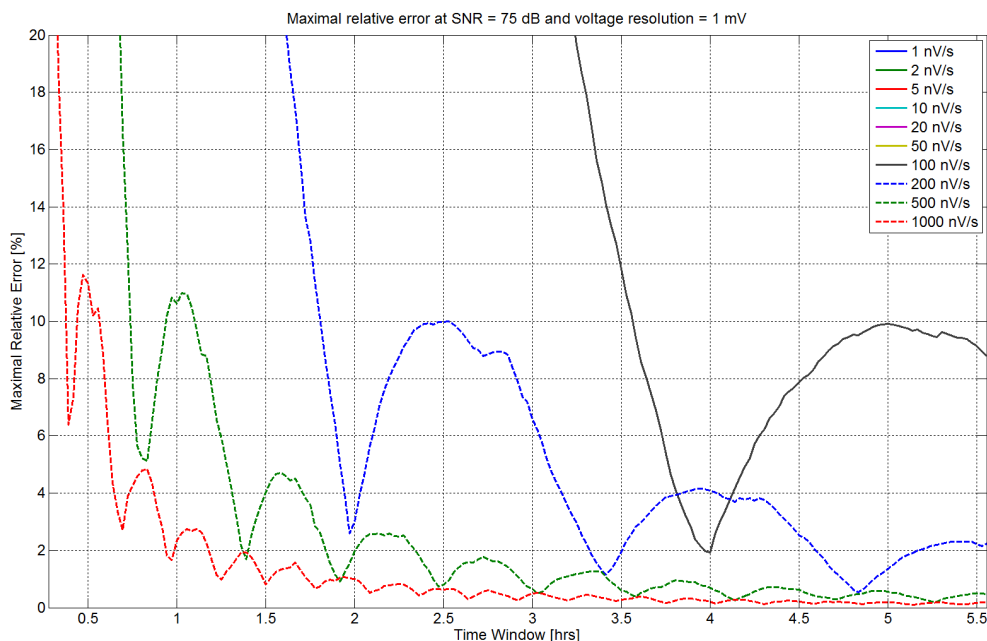


Figure 2.4: Zoomed part of Figure 2.3.

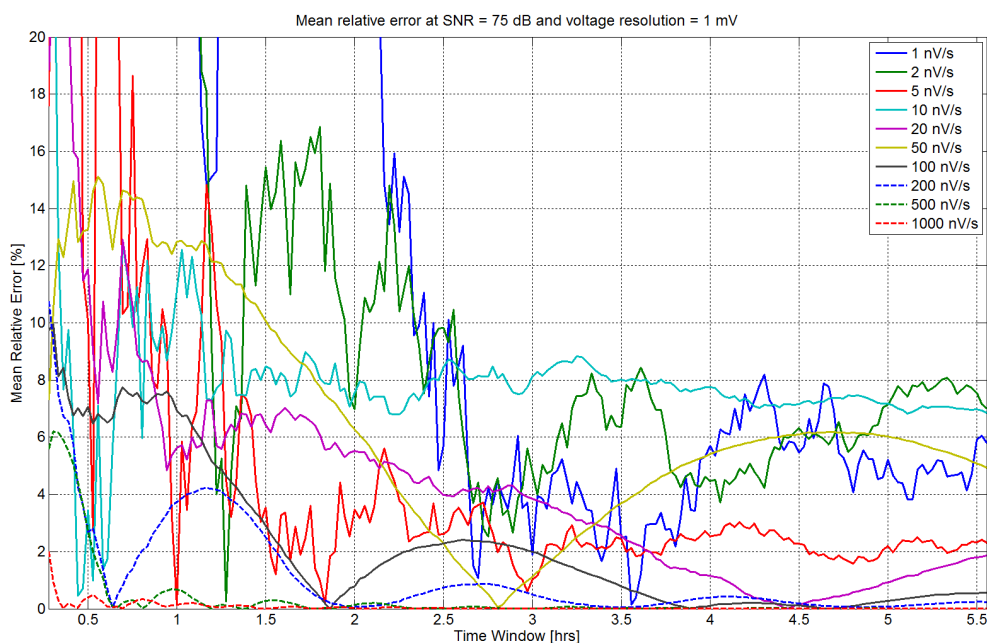


Figure 2.5: The mean relative error, zoomed to the same part as Figure 2.4.

In Figure 2.6, on the right side, the maximal relative error for different SNR is represented



in relation to the window time. Remarkable is that the higher SNR, which is usually considered as better measurement, causes a bigger error than the smaller SNR. In addition, the systematic behavior can be figured out for a SNR= 90 dB and SNR=75 dB. Only the SNR=60 dB does not suffer from this systematic behavior.

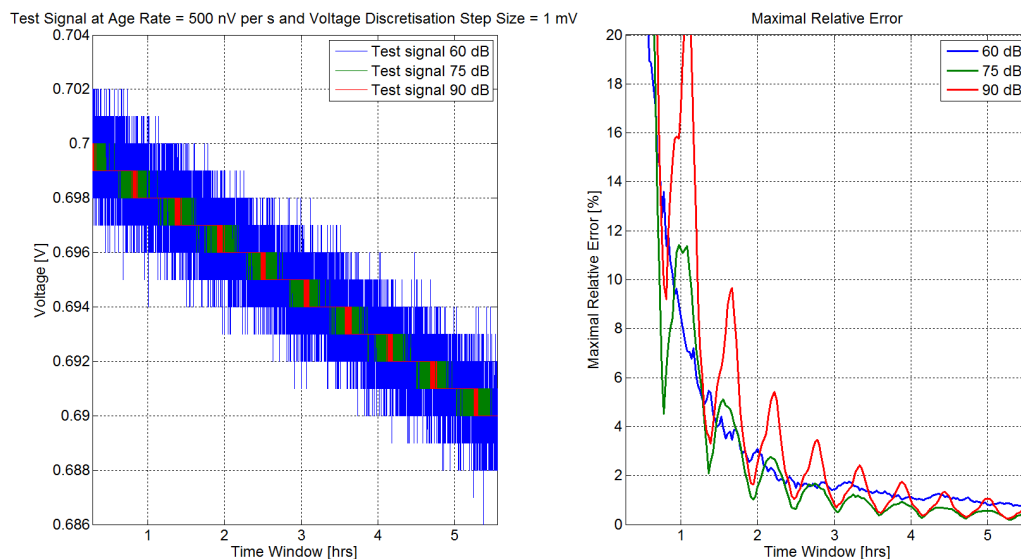


Figure 2.6: An artificial voltage signal at different SNR and its maximal, relative error.

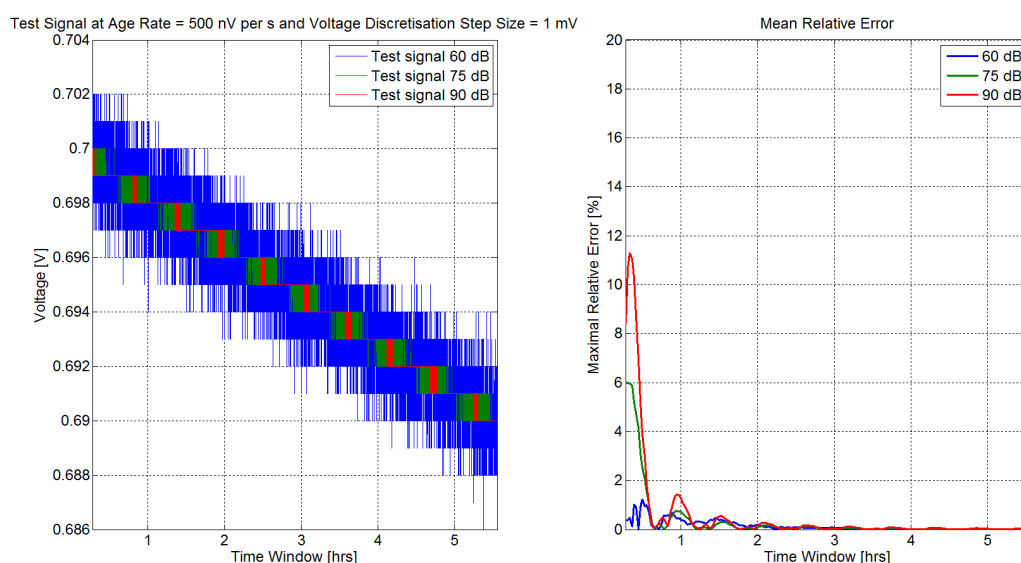


Figure 2.7: An artificial voltage signal at different SNR and its maximal, relative error.

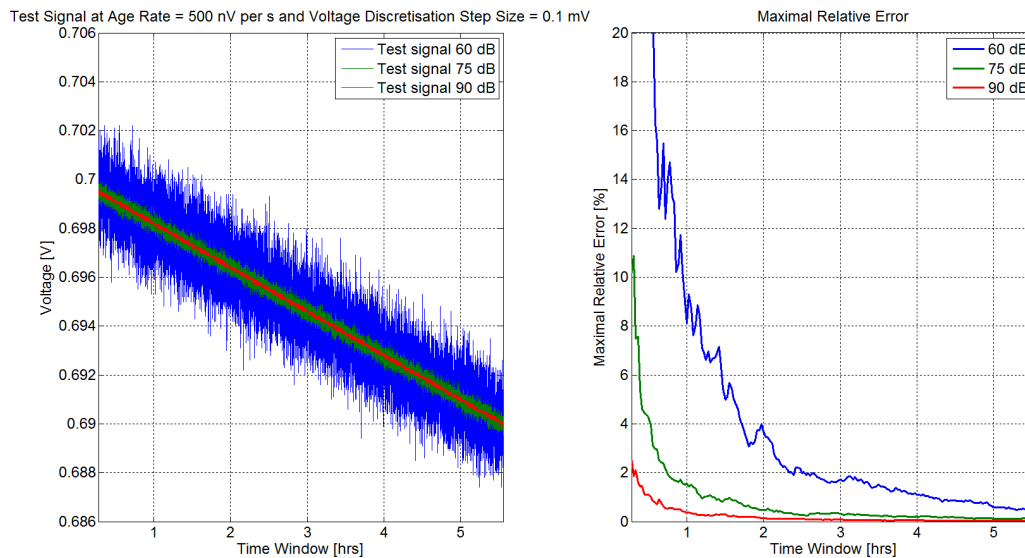
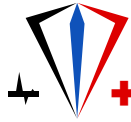
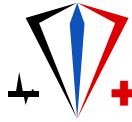


Figure 2.8: An artificial voltage signal at different SNR and its maximal, relative error.

The reason can be found on the left side. This side shows the part of the different test signals, which were used to obtain the result. The red trend, SNR=90 dB, forms clear steps and voltage plateaus, as already noticed in the beginning of this investigation. The time interval includes different parts of these plateaus, which do not represent the correct ageing rate. The occurring maxima in Figure 2.6, right side, are related to adverse overlapping of the time windows and the voltage plateaus. The minima are related to favorable overlapping. With increasing time window, the problem decreases due to the better averaged ageing rate. The blue trend, SNR=60 dB, does not have such problems, because the bigger noise causes a bigger standard deviation. This standard deviation includes more discrete voltage levels. In this case, it is helpful for finding a more correct ageing rate by using a time window, because more information for the statistical method of least square is provided.

Figure 2.7 shows the same artificial voltage signal as Figure 2.6, but on the right side, it presents the mean relative error related to the window size. Compared to Figure 2.6, the mean relative error is significant smaller than the maximum relative error, but it still suffers from the same effects. A higher SNR causes a bigger error and the error changes in a systematic way. A more averaged ageing rate improves the result, but still suffers from the systematic error of the 1 mV discretization steps.

Figure 2.8 shows on the left side the same voltage signal for different SNR, but with a higher voltage resolution and on the right side the maximum relative error for different SNR related to the time window size. Compare to Figure 2.6, the result does not improve for a SNR=60 dB, which is not surprising, because in Figure 2.6, the artificial voltage provided already a real noisy behavior and the result includes the benefit of the statistical effect already. The results for SNR=75 dB and SNR=90 dB are more interesting. In Figure 2.8, they show as well a noisy behavior and in the case of a voltage steps equal to 0.1 mV, the higher SNR causes better result as it would be expected. The reason is that the least square method now forms a better lin-



ear fit and the ageing rate can be found more precisely. Instead of systematic wrong voltage plateaus, the Gaussian noise provides additional input for the averaged ageing rate and the ageing rate can be found below a maximal relative error of 2% within a time window of one hour for 500  $nV/s$  ageing rate at SNR=75  $dB$ .

## 2.1.5 conclusion

In order to find and investigate the degradation of a fuel cell, it is necessary to identify the ageing rate correctly. The investigation above shows that a voltage resolution of 1  $mV$  might be too small and causes unnecessary sizes of time windows to investigate the ageing rate. It suffers from systematic error and increasing the SNR only increases this problems. A decreases in measurement quality or a lower SNR seems to help with this issue in the first place. Unfortunately, the voltage of a fuel cell is one of the best indicators of the fuel cell state: decreasing the measurement quality makes it more difficult to use the cell or stack voltage as state indicator, which might cause additional costs for additional sensor instead of using the available information. In addition, lower ageing rates are difficult to detect. Investigating only the stack voltage instead the cell voltage solves this problem partially, but reduces the opportunities of detecting fast decreasing cell voltages. Increasing the time window for the averaged ageing rate and repeating this for several time to have an overall averaged ageing rate, improves the result but increases the measuring time and does not solve the systematic error, caused by the voltage resolution.

In the end, it is recommended to use equipment with higher discrete voltage resolution to improve the correct detection of the ageing rate.

## 2.1.6 Impact of ageing rates

The project data were measured with a voltage resolution of 1  $mV$  and a SNR higher than 75  $dB$ . According to the test protocol, fast cycling was used to amplify the ageing of the stacks. For example, the current density stays only for 2 hours and 15 minutes at 0.35  $A/mm^2$  and the fuel cell stack could hardly reach the steady state. Figure 2.9 shows the difficulty. The Fuel cell stack cannot reach the steady state fast enough and in the end, there is only a 40 minutes time window to find a correct ageing rate. Unfortunately, the investigation of the ageing rate detection shows that this steady state time is too short to find directly a small ageing rate inside the voltage. Using the stack voltage instead of the cell voltage leads to a higher, absolute ageing rate, because all ageing rates of the cells are summed up inside the stack voltage. This decreases the influence of the issue, but during the project, even the ageing rate of the stack voltage were only 20  $nV/s$  (for the Dantherm Sapphire 2 stack).The investigation shows that a strategy, using average approaches, is required to find the correct ageing rate. In this case, within one single constant operation interval, the ageing rate can only be found by chance and not systematically. On the other hand, there is no other data than the short windowed data. For that reason, a procedure was developed to find the best estimation of the ageing rate within the short time window and to weight found ageing rates.

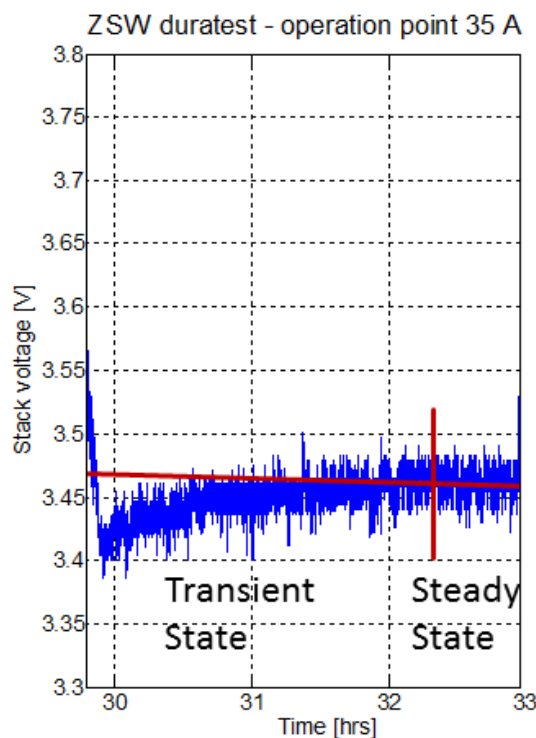


Figure 2.9: A general time interval of ZWS data at 35 A.

### 2.1.7 Ageing Rate and Standard Deviation Detection

The following section deals with an approach to value the quality of the linear fit. Due to the slow decrease of the voltage in comparable conditions, the simplest way to detect it is a linear fit on a feasible time interval. In the previous section, it has been shown that this time interval is not available for some current levels and an average approach is required. Therefore the calculated ageing rates might be poor a estimation of the real ageing rate. A way to test the quality of the ageing rate is to investigate, how well a fit really represents the data and how many values are used for the calculation of a fit.

The procedure needs a minimum and maximum window size, which form a search interval. Inside this interval, several linear fits are done and evaluated. The minimum window size ensures to use enough values in order to decrease the impact of noise and outliers on the linear fit. The maximum window has to be as large as possible to get the best possible amount of values for finding a well averaged fit. It is not useful to directly apply the maximum possible window, because effects like oscillation and outliers might influence the result negatively and only one estimation would be available. Using a window smaller than the short interval gives several estimations of the ageing rate and provide an averaged, correlated mean ageing rate. According to the investigation of the ageing rate detection, this kind of average value improves the ageing rate detection.

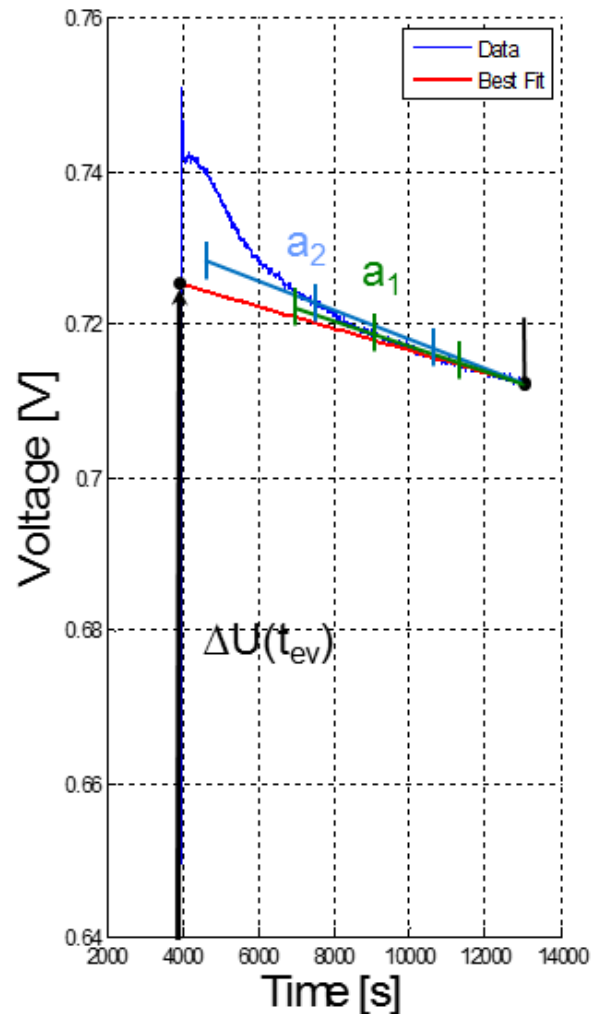
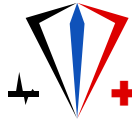


Figure 2.10: A fuel cell voltage response on a change of operation together with different steps of the ageing rate detection.

If there is not enough data according to a predefined maximum window length, the ageing rate detection does nothing. Otherwise, the procedure works the following way:

- First, a set of data with a decided maximum window length is given to the age rate detection. When a new measurement occurs, the maximum window forgets the oldest data point and adds the new one.
- Second, the detection starts from the last point of the data, but considers a minimum amount of values in order to sustain influences of noise. Figure 2.10 shows such a window (green).
- Third, the fit is calculated, using the least square approach. The gradient of the found fit  $a_1$  is kept.
- Fourth, the found fit gets separated in three smaller windows with equal size and each windows counts the number of values above and below the found fit. A good fit would





lead to 50% of the values below and 50% above for each of the three windows. Due to the least square method, only the complete interval of  $a_1$  fulfills this rule for every case and the distribution inside the smaller windows is a possibility to prove the quality of the linear fit. The method can sustain a decent amount of oscillations and outliers.

- The Fifth step is to calculate a mean of difference from the expected 50% over the three windows.

This procedure is repeated several times for different window sizes (e.g. Figure 2.10), starting at a predefined minimum window size and ending with the maximum window size. Whenever a mean relation difference closer to the best result of 50%, the ageing rate replaces the last found ageing rate and saves the result as best fit (cp. Figure 2.10).

When a new value is available, the procedure is repeated. In this way, every point gets its own estimation of the ageing rate, when the data to analyze is bigger than the maximum window. The distribution difference is used as criteria in order to weight the found ageing rates. A good fit, with 50%-50% distribution in all three control windows leads to a maximum weight of 0.5. In addition, the number of values in relation to the maximum window size are used as criteria. If the best fit interval is equal to the maximum window, which represents the most statistically healthy fit, the maximum weight of 0.5 is obtained. Both weights form a 1, which represent 100% of the found ageing rate will be considered for further investigations. The weights are saved along with the detected ageing rates in order to apply it for an overall mean ageing rate. The procedure gives an estimation of ageing rate for each new point.

Beside the ageing rate, the standard deviation of the voltage is calculated and saved in the same way as the ageing rate. The standard deviation can only be calculated after ageing trend is subtracted from the voltage. Otherwise, the ageing trend increases the standard deviation in relation to its gradient and causes a systematic error, which can vary by the situational ageing rates.

In addition, a transient free start voltage is calculated for every found fit and can be used to achieve a  $\Delta U(t_{ev})$ , the difference to the voltage before the change of operation (cp. Figure 2.10).

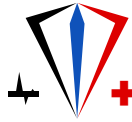
## 2.2 Evaluation of the prognosis

This section is confidential due to the patent process.

## 2.3 Data used

This section is partially confidential due to the patent process.

A detailed description of the data can be found in other deliverables. The algorithm was developed on the 2160 hours duratest from ZSW and validated on the 2850 hours Sapphire 2



data. In addition, these data were used by an Adaptive Neuro-Fuzzy Inference Systems (ANFIS).

## 2.4 Prediction

This section is confidential due to the patent process.

## 2.5 Algorithm for the system

The final step would be an executable, created by Matlab Compiler. The principle would be to copy this executable onto a windows industrial computer of a fuel cell system and install the free Matlab executable library. Depending on the preferences of the system producer, the executable can be started manually by a user or frequently by the fuel cell control.

### 2.5.1 Architecture

The architecture is simple and executables can be used on different systems, as long as the Matlab library can be installed and the OS is able to start executables. However, there are some steps before building the executable, which are important for the usability.

The most important step is the decision for an interface or how the measured parameters (current, voltage and additional correction parameters) are taken by the algorithm. For example, the running control system can save the measured data in a txt-file and start the executable time after time. The executable can import different file formats (txt or csv) and use different data structures (e.g. first data column is current and second column is voltage), but it has to be implemented before the executable is generated and cannot be changed afterwards. The procedure would be to define the file format and the data structure and tell the fuel cell control system to save the measured data in that specified way to the folder of the executable.

An important information for the algorithm is the future current profile, because it supplies the calculation of the remaining useful lifetime, how the future will look like according to the planned operation strategy. This profile has to be loaded every time the executable is run or it could be implemented inside the executable, which makes it easier to apply the algorithm. On the other hand, the algorithm can be only used for that implemented profile, which is an additional and properly unnecessary constrain. The last thing to specify, would be the output. The simplest way could be a single number, saved in a file and loaded by the fuel cell system control. Displaying the number in an additional output window from the executable is a possibility as well. Another way could be a plot with the actual, measured data and the estimated trend. The complexity of the output can be increased in an arbitrary way, but should be adjusted to system producer and customer needs.



## 2.6 Conclusion

This section is partially confidential due to the patent process.

The results of the algorithm are very promising. A relative error of 2.3% estimated over 1900 hours into the future for ZSW duratest data done in a lab environment and relative error of 6.7% estimated over 2580 hours into the future for Dantherm Sapphire 2 data done in a fuel cell system shows a high precision, even after several 100 of hours. For the general case of  $\mu$ CHP systems, were a normal and not an accelerated ageing profile is applied, the results should be even better. In addition, the applied ANFIS approach provides an optimization potential for the algorithm and even a possibility to use the model in another way.

In the end, the results are very satisfying and further investigations would improve the practical use of the algorithm.



# Bibliography

- [1] Elodie Lechartier, Elie Laffly, Marie-Cécile Péra, Rafael Gouriveau, Daniel Hissel, and Nouredine Zerhouni. Proton exchange membrane fuel cell behavioral model suitable for prognostics. *International Journal of Hydrogen Energy*, 40(26):8384 – 8397, 2015.
- [2] D-code - dcdc converter-based diagnostics for pem systems; <https://dcode.eifer.kit.edu/>.



## **Annex 1 : Labview documentation**

# Prognostics program documentation

---



The LabVIEW program consists of three main functions, called projects in the following.

The first part of this documentation is dedicated to explaining the purpose of these functions. The second one will allow the user to look into the projects in details.

## Table of Contents

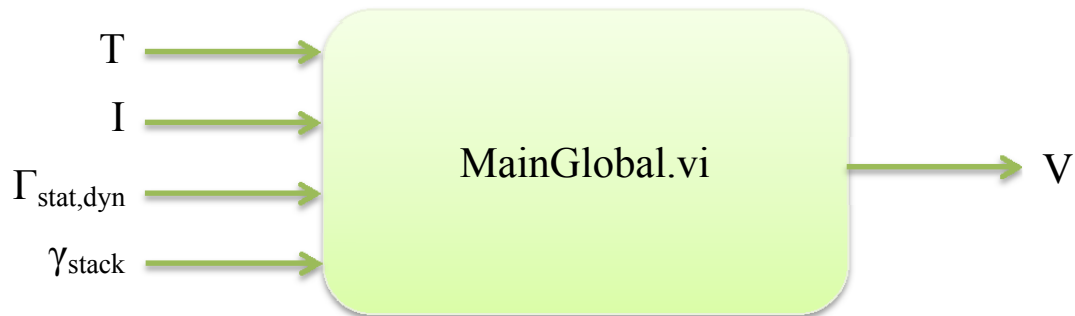
1.	Explanation of main functions .....	3
1.1	Project 1: Voltage estimation - <i>ModeleGlobal_EvalV.lvproj</i> .....	3
1.1.1	Overview of the main function of the project.....	3
1.1.2	Use of the main VI of the project .....	4
1.2	Project 2: Polarization estimation - <i>EvalPola.lvproj</i> .....	6
1.2.1	Overview of the main function of the project.....	6
1.2.2	1.1.2 Use of the main VI of the project .....	6
1.3	Project 3: Updating procedure <i>UpdatingProcedure.lvproj</i> .....	8
1.3.1	Overview of the main function of the project.....	8
1.3.2	Use of the main VI of the project .....	8
1.4	Project 4: Updating procedure <i>UpdatingProcedure.lvproj</i> .....	10
1.4.1	Overview of the main function of the project.....	10
1.4.2	Use of the main VI of the project .....	10
2.	Detailed explanation of the projects .....	12
2.1	Project 1 - <i>ModeleGlobal_EvalV.lvproj</i> .....	12
2.1.1	Overview of the Project Explorer .....	12
2.1.2	Structure and functioning of <i>MainGlobal.vi</i> .....	13
2.1.3	Detailed explanation of sub VI <i>SimulationExp.vi</i> .....	14
2.2	Project 2 - <i>EvalPola.lvproj</i> .....	15
2.2.1	Overview of the Project Explorer .....	15
2.2.2	Structure and functioning of <i>Main.vi</i> .....	15
2.3	Project 3 - <i>UpdatingProcedure.lvproj</i> .....	16
2.3.1	Overview of the Project Explorer .....	16
2.3.2	Structure and functioning of <i>Main.vi</i> .....	17
2.3.3	Detailed explanation of sub VI <i>Statique.vi</i> .....	18
3.	How to run the program .....	20

# 1. Explanation of main functions

## 1.1 Project 1: Voltage estimation - *ModeleGlobal\_EvalV.lvproj*

### 1.1.1 Overview of the main function of the project

The purpose of this project is to evaluate the voltage at a time  $t$ .



Inputs:

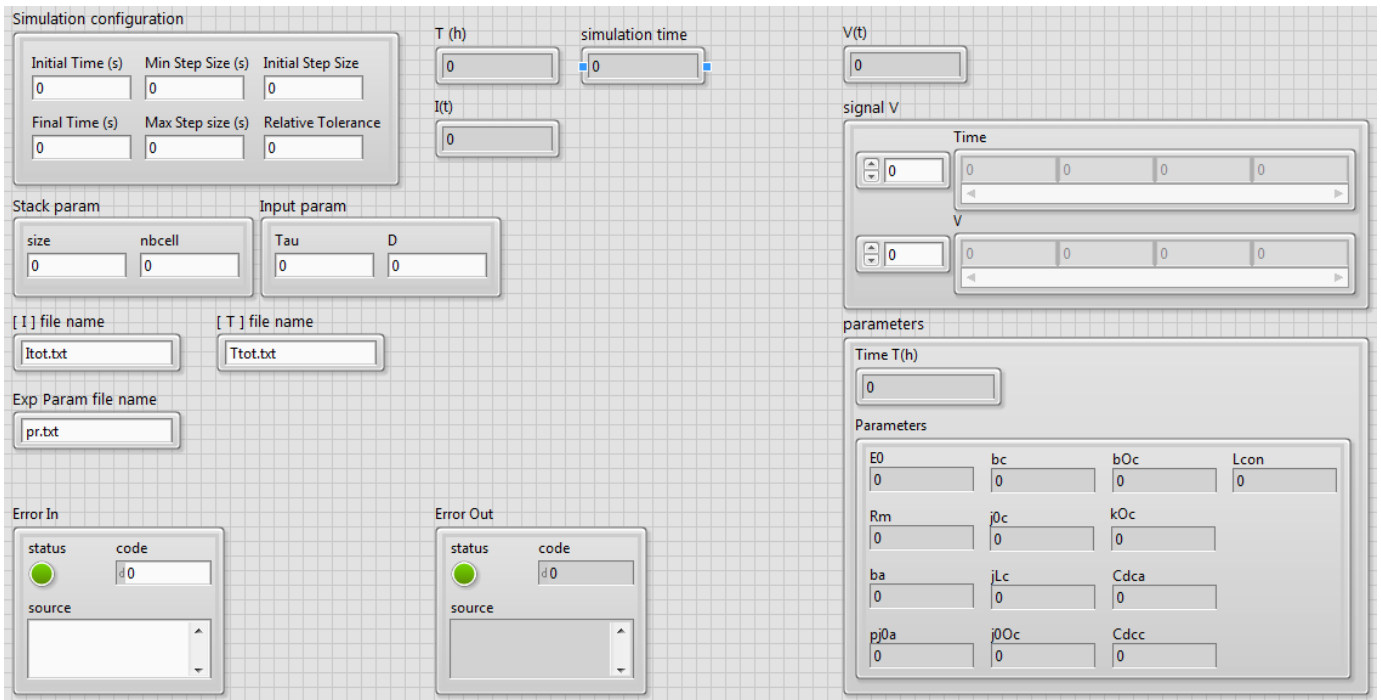
- $T$  the aging time in hours (array)
- $I$  the current (array corresponding to  $T$ )
- $\Gamma_{stat,dyn}$  exponential parameters (fitting of static and dynamic parameters)
- $\gamma_{stack}$  stack characteristics (active area and number of cells)

Output:

- $V$  voltage (array corresponding to  $T$ )

## 1.1.2 Use of the main VI of the project

Here is the Front panel of *MainGlobal.vi*:



Control elements in this front panel are:

- *Simulation configuration*: It is a cluster of numeric controls that will configure the control and simulation loop. User can add other parameters and wire them to the loop.
- *Stack param*: It is a cluster of numeric controls that corresponds to  $\gamma_{\text{stack}}$  values.
- *Input param*: It is a cluster that contains two numeric controls; *Tau* is the time constant of the low-pass filter and *D* is the gap from  $t_0$  that will be initially fixed at 0.022 (can be changed).
- *[I] file name*: It is a string control of the text file name that contains **I** array data. The array should be stored in the form of a column vector
- *[T] file name*: It is a string control of the text file name that contains **T** array data. This array should also be stored in the form of a column vector and its number of rows should be equal to the number of rows of **I**.

- *Exp Param file name*: It is a string control of the text file name that contains  $\Gamma_{\text{stat,dyn}}$  (exponential parameters). The storage should be in the following order (from the 1<sup>st</sup> row to the last one):

$\Gamma_{E0}$   
 $\Gamma_{Rm}$   
 $\Gamma_{ba}$   
 $\Gamma_{j0a}$   
 $\Gamma_{bc}$   
 $\Gamma_{j0c}$   
 $\Gamma_{jLc}$   
 $\Gamma_{j0Oc}$   
 $\Gamma_{bOc}$   
 $\Gamma_{kOc}$   
 $\Gamma_{Cdca}$   
 $\Gamma_{Cdcc}$   
 $\Gamma_{Lcon}$

Amplitudes should be in the first column and damping in the second.

These parameters are already stored by the third project *UpdatingProcedure.lvproj*.

In this front panel, indicator elements are the following:

-  $T(h)$ : It is a numeric indicator that shows the variation of the aging time  $\mathbf{T}$  through the simulation.

-  $I(t)$ : It is a numeric indicator that shows the variation of the current  $\mathbf{I}$  through the simulation.

- *simulation time*: It's a numeric indicator that shows the variation of the simulation time generated by the control and simulation loop.

-  $V(t)$ : It is a numeric indicator that shows the variation of the voltage  $\mathbf{V}$  through the simulation.

- *signal V*: It is a cluster of two array indicators; *Time* shows the simulation time array and *V* shows the voltage  $\mathbf{V}$ . These results are displayed at the end of the simulation.

- *parameters*: It is a cluster of numeric indicators that show, through the simulation, the variation of the time  $T(h)$  and the parameters values at this time.

## 1.2 Project 2: Polarization estimation - *EvalPola.lvproj*

### 1.2.1 Overview of the main function of the project

The aim of this project is to estimate a polarization curve.



Inputs:

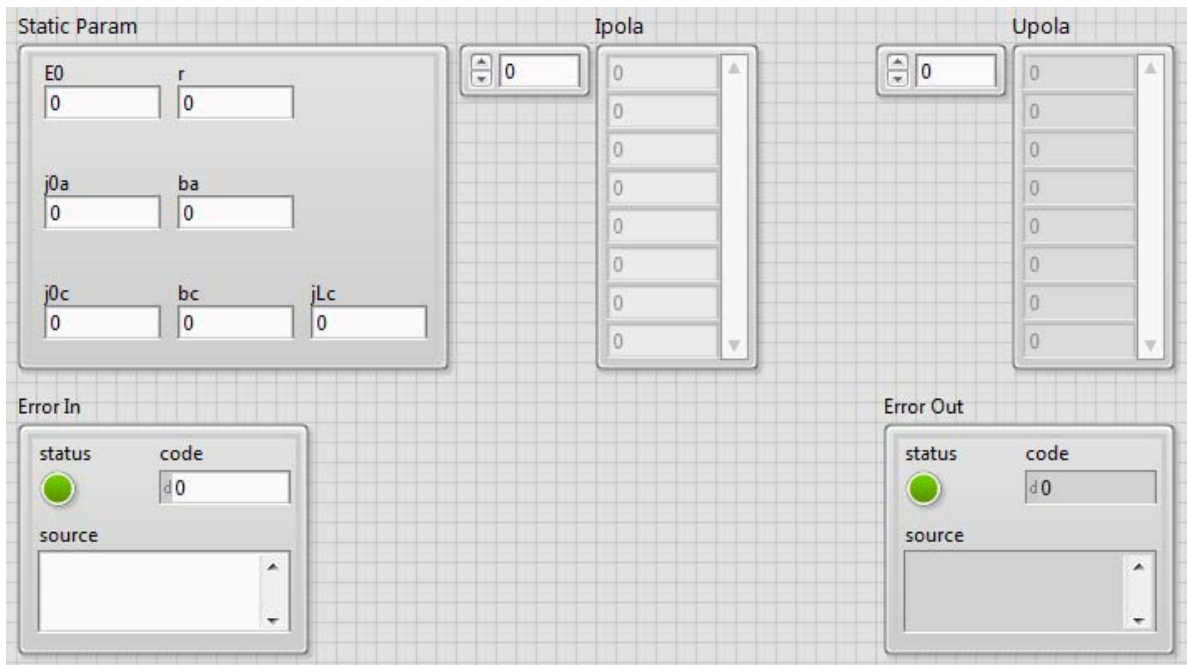
- I** current in the form of array data
- $\theta_{stat}$**  static parameters (one could use the results of the third project)

Output:

- V** array of voltage values

### 1.2.2 Use of the main VI of the project

The front panel of Main.vi:



In this front panel there are two control elements:

- *Static Param*: It is a cluster of numeric controls. It corresponds to  $\theta_{\text{stat}}$  values. The user could use the exponential parameters  $\Gamma_{\text{stat}}$  obtained by the third project *UpdatingProcedure.lvproj*.

- *Ipola*: It is an array control that correspond to the current  $I$ . This array could be changed into an indicator and wired to a spreadsheet file.

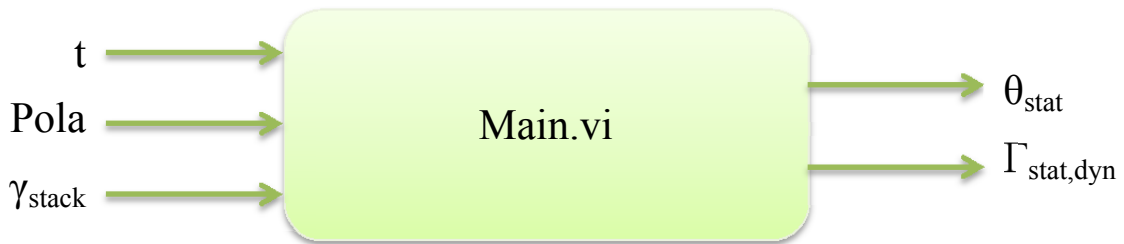
There is one indicator element:

- *Upola*: It's an array indicator that corresponds to the voltage  $V$ .

## 1.3 Project 3: Updating procedure *UpdatingProcedure.lvproj*

### 1.3.1 Overview of the main function of the project

Firstly, this project fits the static model to an experimental polarization curve in order to obtain the best option for the static parameters. When the number of polarization curves fitted is up to three, this project is able to give the parameters of the exponential functions for each parameter.



Inputs:

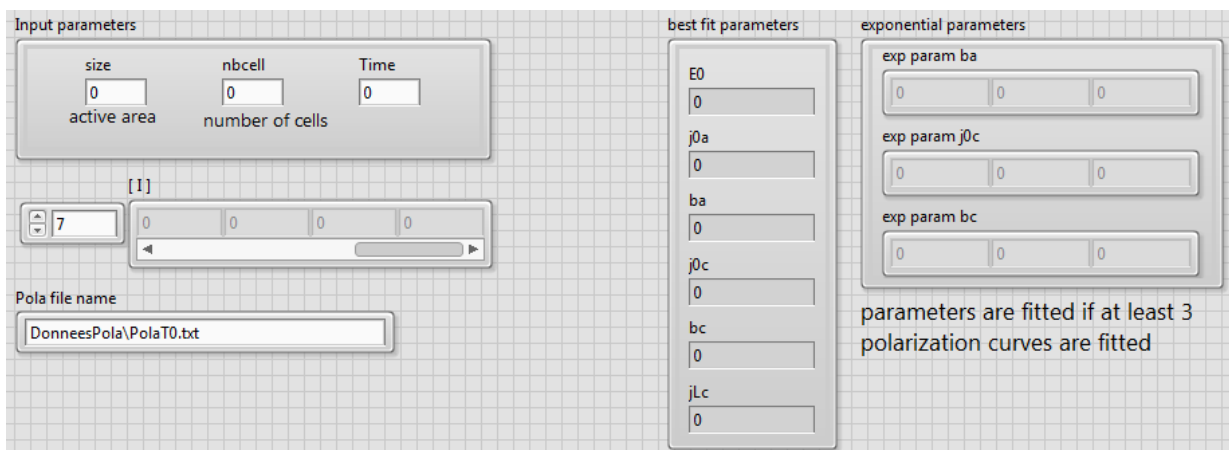
- t** time
- Pola** pola data at time t
- $\gamma_{stack}$**  stack characteristics (number of cells and active area)

Outputs:

- $\theta_{stat}$**  static parameters at time t
- $\Gamma_{stat,dyn}$**  exponential parameters of static and dynamic parameters fitting

### 1.3.2 Use of the main VI of the project

Here is an overview of the front panel of Main.vi



The control elements that the user would have to enter are the following:

- *Input parameters*: It is a cluster of numeric controls of stack characteristics  $\gamma_{\text{stack}}$  and time  $t$ .

- *[I]*: It is a one dimension array control that the user has to fill with the current values that the system were stabilized during the polarization curve.

- *Pola file name*: It is a string control of the text file name that contains **Pola** data at time  $t$ .

The user could see the results in the following indicators:

- *best fit parameters*: It shows the values of  $\theta_{\text{stat}}$  at time  $t$  in a cluster of numeric indicators.

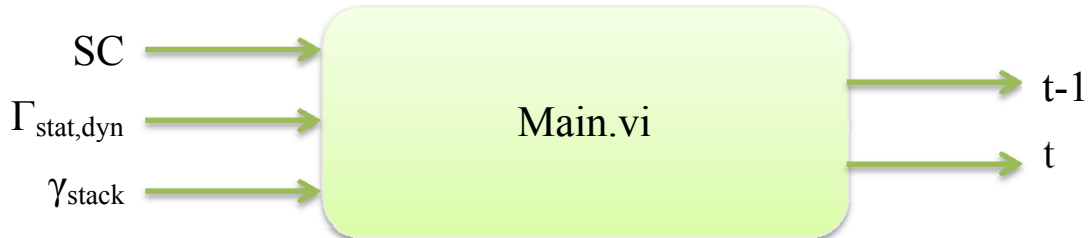
- *exponential parameters*: it is a cluster of array indicators that shows  $\Gamma_{\text{ba}}$ ,  $\Gamma_{\text{j0c}}$  and  $\Gamma_{\text{bc}}$ . The first element of the array would be the amplitude and the second would be the damping. The user would get to see it only after the third polarization curve fitting.



## 1.4 Project 4: RUL estimation *ModeleGlobal\_EvalV.lvproj*

### 1.4.1 Overview of the main function of the project

This project is a replicate of the second one that will give the time at which the threshold for the RUL is hit. This threshold is defined as 0.6 V/cell at 35A.



Inputs:

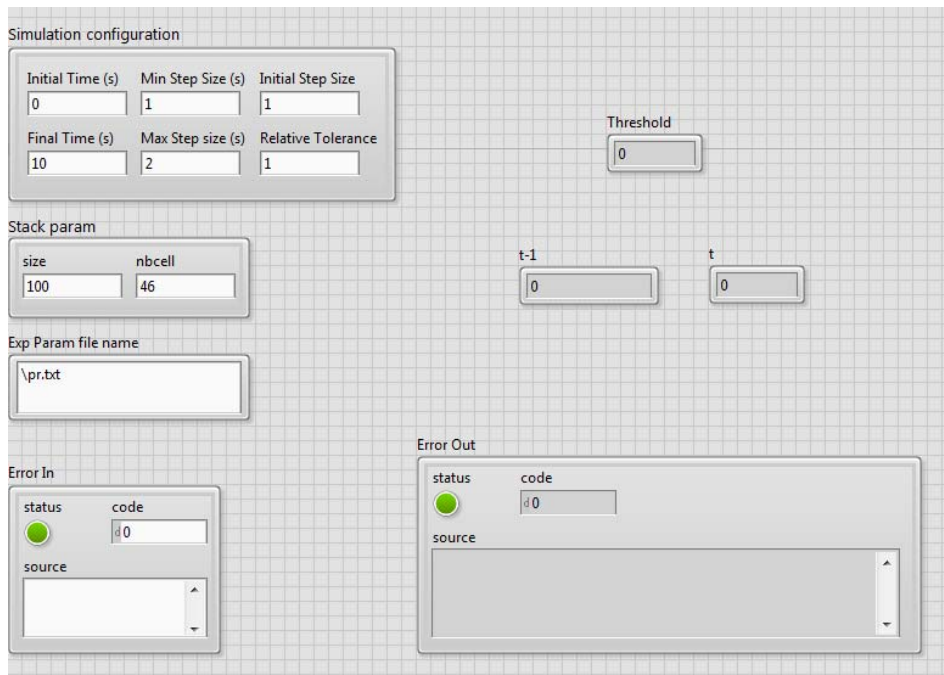
- SC** simulation configuration
- $\Gamma_{stat,dyn}$**  exponential parameters of static and dynamic parameters fitting
- $\gamma_{stack}$**  stack characteristics (number of cells and active area)

Outputs:

- t-1** last time with the voltage higher than the threshold
- t** first time with the voltage lower than the threshold

### 1.4.2 Use of the main VI of the project

Here is an overview of the front panel of Main.vi



The control elements that the user would have to enter are the following:

- *Simulation configuration*: It is a cluster of numeric controls if the time for the simulation.

- *Stack Param*: It is a cluster of numeric controls for the values of the stack characteristics  $\gamma_{\text{stack}}$ .

- *Exp Param file name*: It is a cluster string control of the text file name that contains the exponential parameters  $\Gamma_{\text{stat,dyn}}$ .

- *Pola file name*: It is a string control of the text file name that contains **Pola** data at time  $t$ .

The user could see the results in the following indicators:

- *Threshold*: It shows the values of the threshold.

- *t-1*: It shows the values of the last time at which the threshold was not hit.

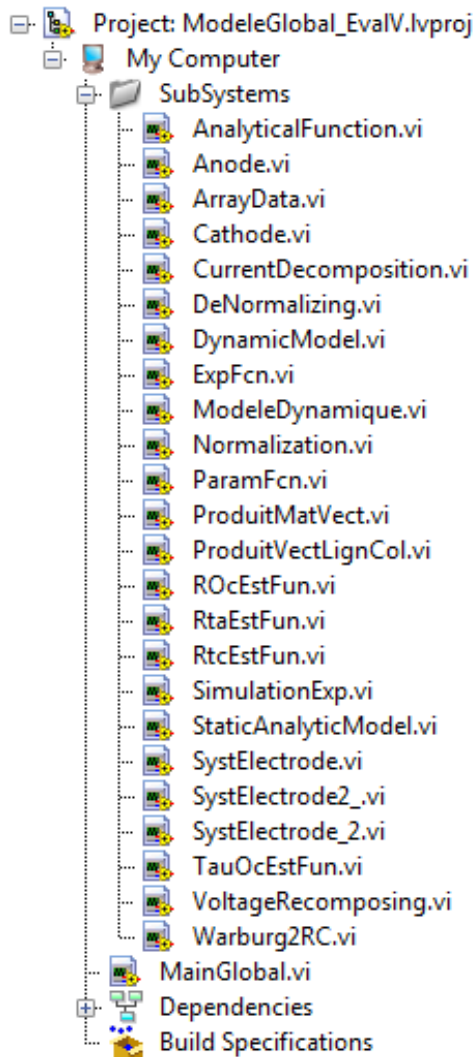
- *t*: It shows the values of the first time at which the threshold was hit.

The RUL will be a time between the *t-1* and the *t*.

## 2. Detailed explanation of the projects

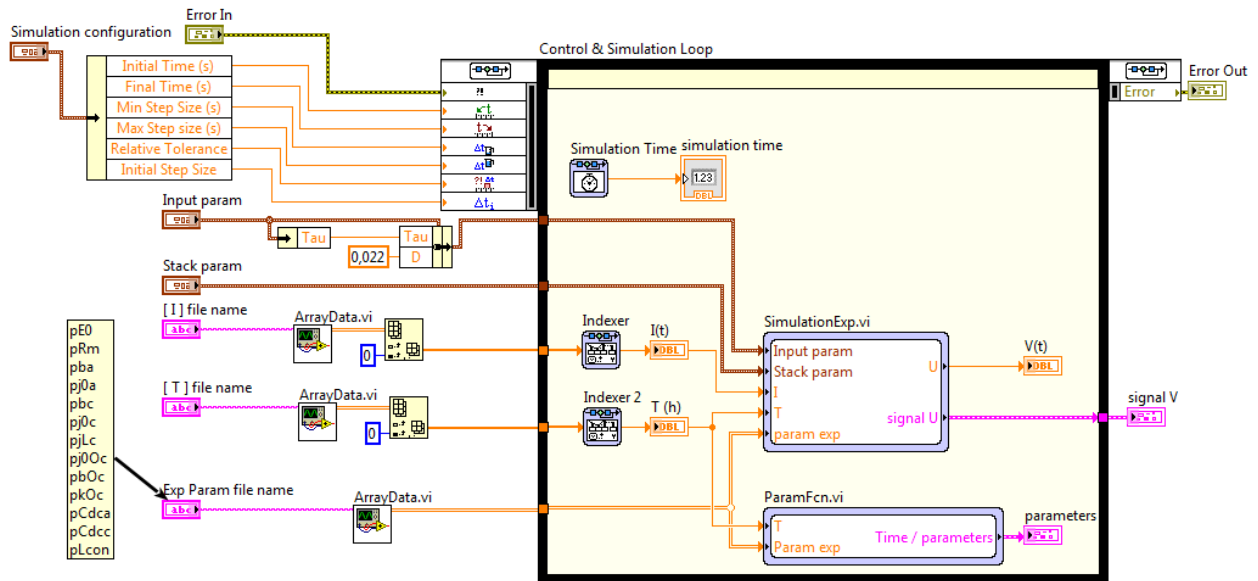
### 2.1 Project 1 - *ModeleGlobal\_EvalV.lvproj*

#### 2.1.1 Overview of the Project Explorer



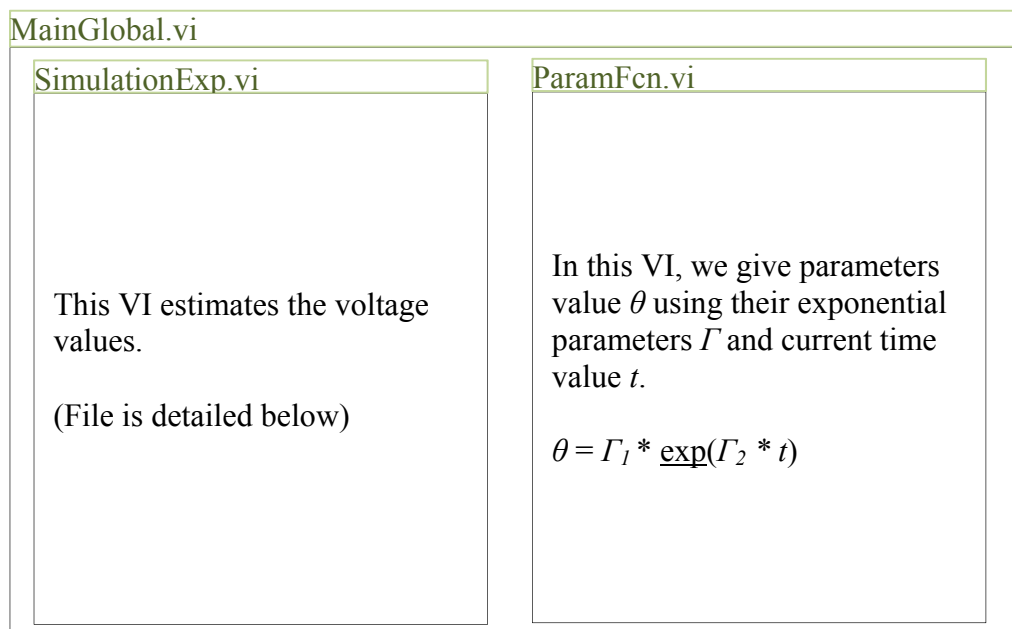
## 2.1.2 Structure and functioning of *MainGlobal.vi*

Here is the block diagram of the VI:



As we can see in the figure above, *MainGlobal.vi* contains a control and simulation loop. All others \*.vi files are simulation subsystems.

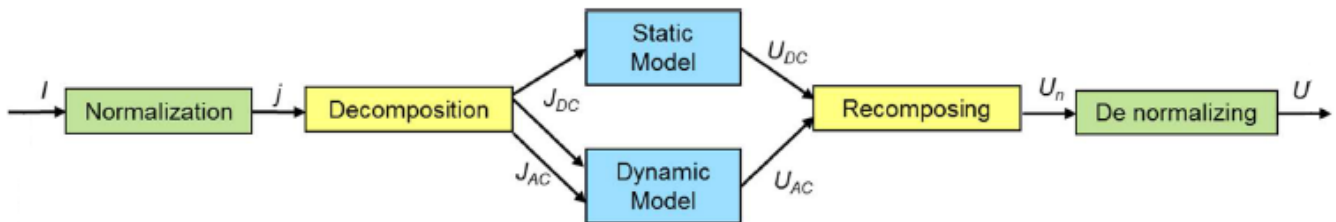
The functioning of this VI and its sub VIs is the following:



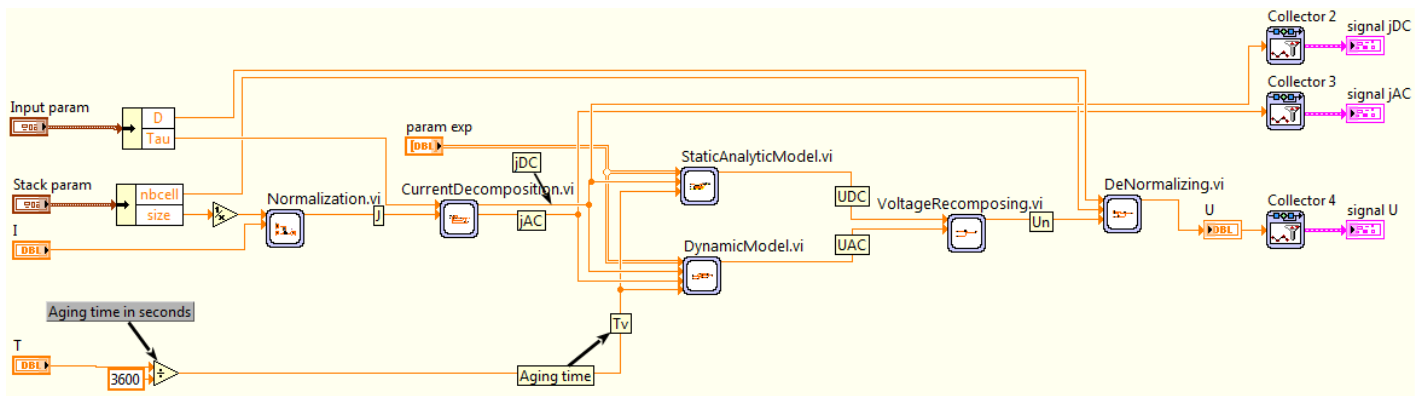
### 2.1.3 Detailed explanation of sub VI *SimulationExp.vi*

In this project, *SimulationExp.vi* follows the physics based behavioural model.

Physics based behavioural model:



Overview of *SimulationExp.vi*:

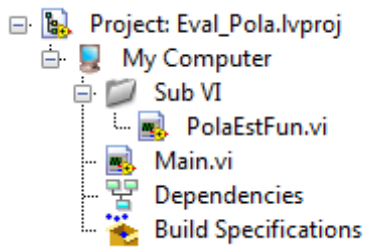


Analogy:

<b>Normalization</b>	↔	<i>Normalization.vi</i>
<b>Decomposition</b>	↔	<i>CurrentDecomposition.vi</i>
<b>Static Model</b>	↔	<i>StaticAnalyticModel.vi</i>
<b>Dynamic Model</b>	↔	<i>DynamicModel.vi</i>
<b>Recomposing</b>	↔	<i>VoltageRecomposing.vi</i>
<b>De normalizing</b>	↔	<i>DeNormalizing.vi</i>

## 2.2 Project 2 - *EvalPola.lvproj*

### 2.2.1 Overview of the Project Explorer

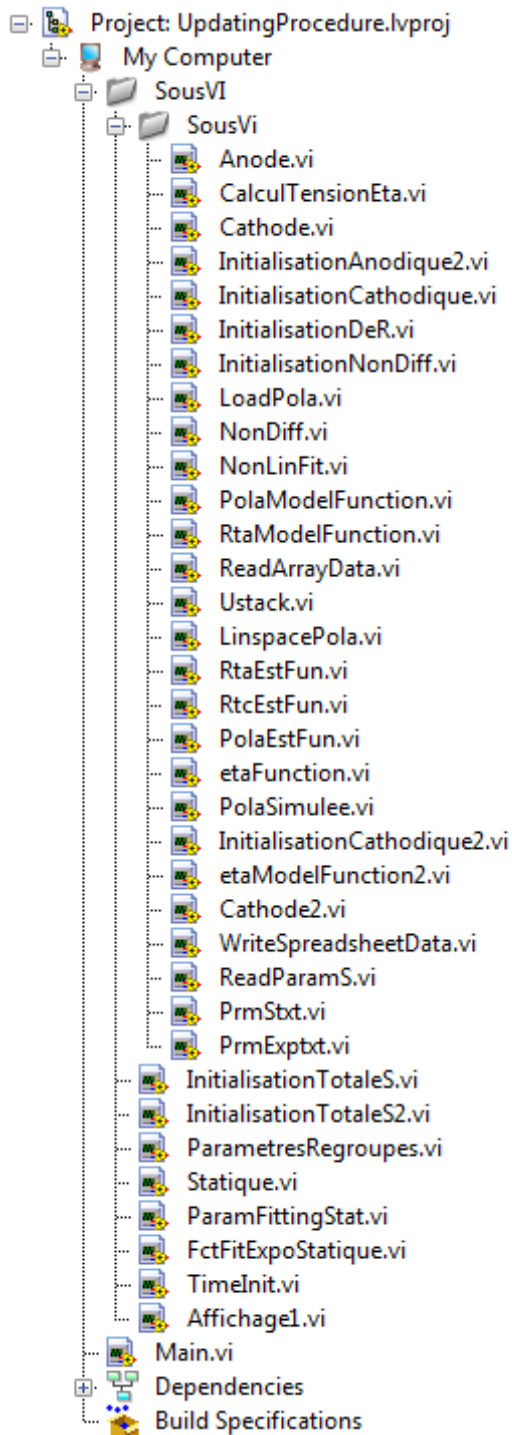


### 2.2.2 Structure and functioning of *Main.vi*

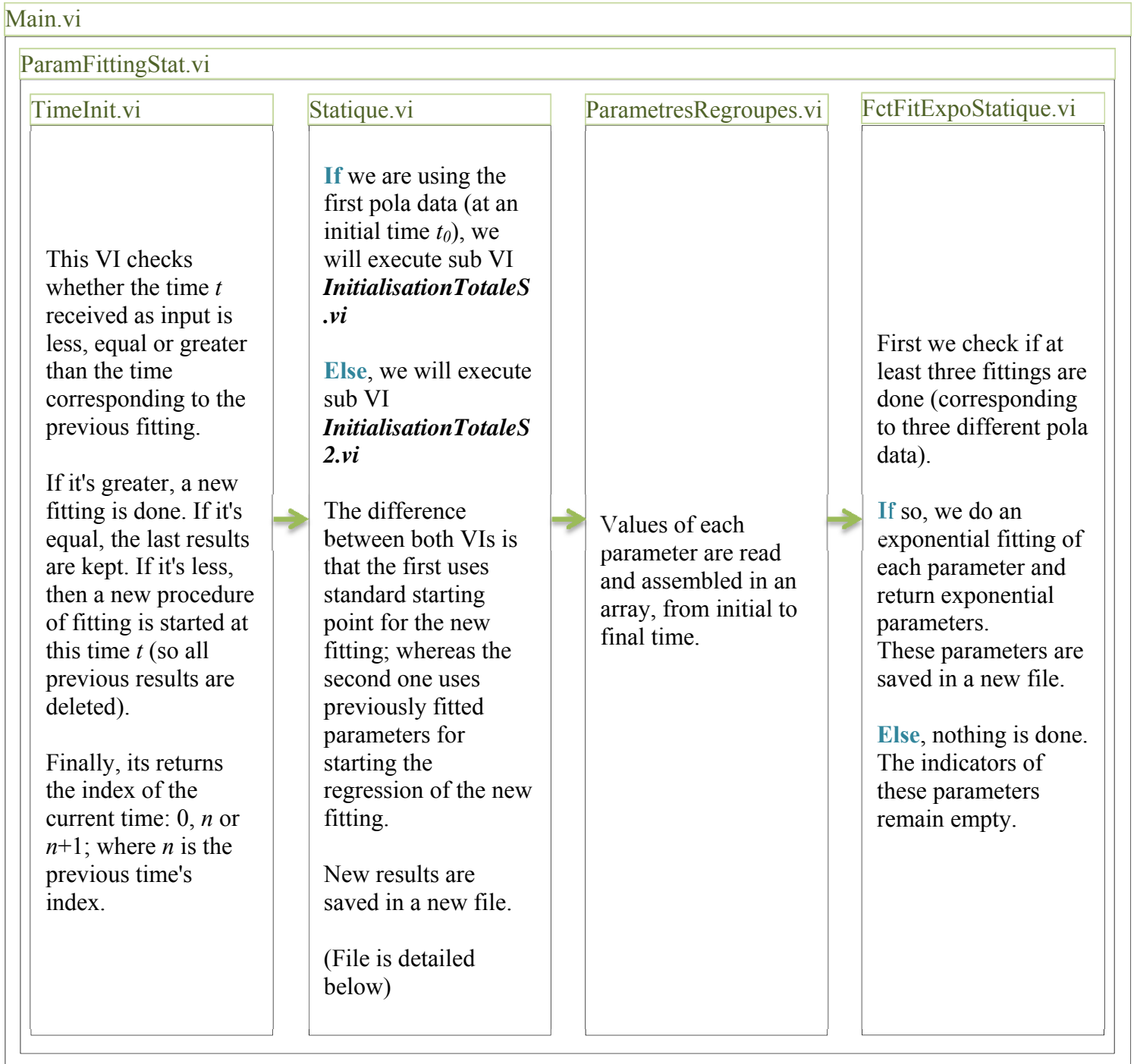
Main.vi		
<table border="1"><tr><td>PolaEstFun.vi</td></tr><tr><td><p>It receives <i>Ipola</i> and <i>Static parameters</i> as inputs and returns <i>Upola</i>.</p><p>It represents the static model function in order to estimate the voltage values under the current solicitation set as input.</p></td></tr></table>	PolaEstFun.vi	<p>It receives <i>Ipola</i> and <i>Static parameters</i> as inputs and returns <i>Upola</i>.</p> <p>It represents the static model function in order to estimate the voltage values under the current solicitation set as input.</p>
PolaEstFun.vi		
<p>It receives <i>Ipola</i> and <i>Static parameters</i> as inputs and returns <i>Upola</i>.</p> <p>It represents the static model function in order to estimate the voltage values under the current solicitation set as input.</p>		

## 2.3 Project 3 - UpdatingProcedure.lvproj

### 2.3.1 Overview of the Project Explorer



### 2.3.2 Structure and functioning of *Main.vi*





### 2.3.3 Detailed explanation of sub VI *Statique.vi*

#### Statique.vi

If we are using the first pola data (at an initial time  $t_0$ ),

#### InitialisationTotaleS.vi

##### NonDiff.vi

**LoadPola.vi** reads pola data and returns current  $I_{pola}$  and voltage  $U_{pola}$  values. It uses stack characteristics and current array that we give as input for polarization.



**InitialisationDeR.vi** reads exponential parameters of  $R_m$  and returns  $r$  at time  $t$ .



**InitialisationNonDiff.vi** does a non-linear curve fitting of  $U_{pola}$  using initially fixed parameters and returns best fitting for  $i_0$ ,  $b$  and  $iL$ . The model equation to fit  $U_{pola}$  is coded in **PolaModelFunction.vi**. For the fitting, we use the sub VI **NonLinFit.vi**, based on Levenberg-Marquardt model.

##### Anode.vi

In this VI, we read  $R_{ta}$  exponential parameters and then return  $R_{ta}$  at  $t$ .



In **InitialisationAnodique2.vi** we do a non-linear curve fitting of  $R_{ta}$  with initially fixed parameters and return the best fitting for  $ba$ . Again, we use **NonLinFit.vi**. And the model equation for this fitting is coded in **RtaModelFunction.vi**.

##### Cathode.vi

Using parameters returned by **NonDiff.vi** and **Anode.vi**, **CalculeTensionEta.vi** returns a voltage  $E_{ta}$ .



Then **InitialisationCathodique.vi** does a non-linear curve fitting of  $E_{ta}$  with initially fixed parameters and returns the best fitting for  $j_0c$ ,  $fbc$  and  $jLc$ . Again, we use **NonLinFit.vi**.

**Else** (we are not doing the first polarization)

## InitialisationTotaleS2.vi

## NonDiff.vi

In this case, we execute **LoadPola.vi**, **InitialisationDeR.vi** and **InitialisationNonDiff.vi** in the same order. The previously fitted values of  $i_0$ ,  $b$  and  $iL$  are used as starting points.

## Anode.vi

In the same way, here we will first read  $R_{ta}$  and return it. Then in **InitialisationAnodique2** we will put last fitting parameters as input and return new ones.

## Cathode2.vi

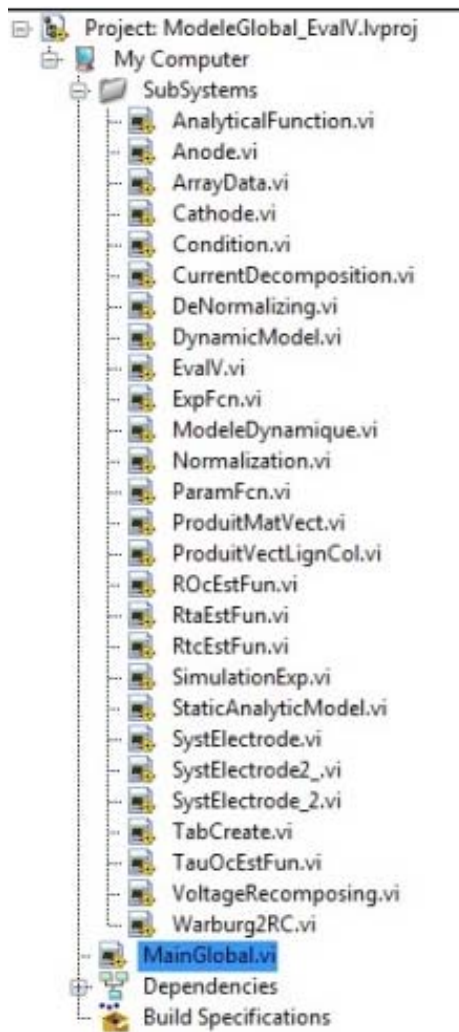
Parameters results obtained by **NonDiff.vi** and **Anode.vi** are imported and create a voltage  $E_{ta}$ .



**InitialisationCathodique2.vi** will do a non-linear curve fitting of  $E_{ta}$  with the parameters  $j_0c$ ,  $bc$  and  $jLc$  obtained by the previous fitting and will return the best fitting for  $j_0c$ ,  $bc$ . As for  $jLc$ , it will remain the same for next fittings. The model equation for this fitting is in **etaModelFunction2.vi**

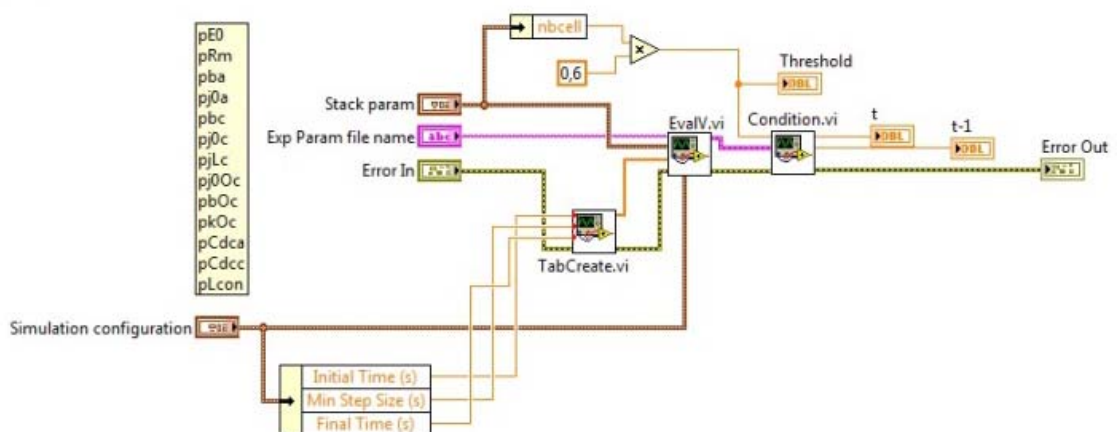
## 2.4 Project 4: RUL estimation *ModeleGlobal\_EvalV.lvproj*

### 2.4.1 Overview of the Project Explorer

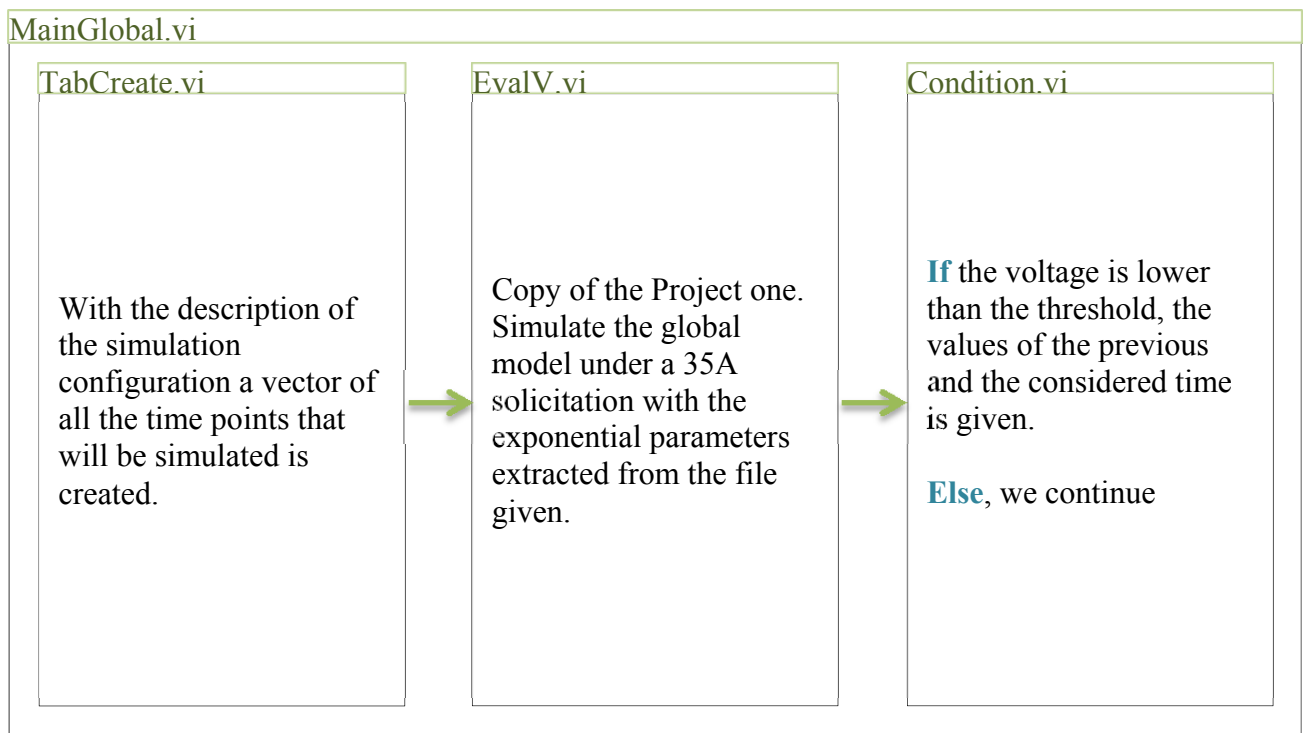


### 2.4.2 Structure and functioning of *MainGlobal.vi*

Here is the block diagram of the VI:



As we can see in the figure above, *MainGlobal.vi* contains a copy of the project 1 and a condition.



### 3. How to run the program

To run one of the projects:

- > go to the main directory
- > open the project's folder
- > open the project by selecting \*.lvproj file
- > In the Project Explorer, the main VI is always stored in My Computer and the others are in virtual folders.
- > enter all controls' values in the main VI's Front Panel
- > run the program

-All text files names could be paths, starting from current VI path.

-Spreadsheet data is always saved in \*.txt files and each values are delimited by *tab* character or *enter* character.